

IMMOBILIZATION OF ZEOLITE CRYSTALS ON SOLID
SUBSTRATES FOR BIOSENSOR APPLICATIONS

A THESIS SUBMITTED TO
THE GRADUATE SCHOOL OF NATURAL AND APPLIED SCIENCES
OF
MIDDLE EAST TECHNICAL UNIVERSITY

BY

SEÇKİN ÖZTÜRK

IN PARTIAL FULFILLMENT OF THE REQUIREMENTS
FOR
THE DEGREE OF MASTER OF SCIENCE
IN
MICRO AND NANOTECHNOLOGY

MAY 2010

Approval of the thesis:

**IMMOBILIZATION OF ZEOLITE CRYSTALS ON SOLID
SUBSTRATES FOR BIOSENSOR APLICATIONS**

submitted by **Seçkin ÖZTÜRK** in partial fulfillment of the requirements for the degree of **Master of Science in Micro and Nano Technology Department, Middle East Technical University** by,

Prof. Dr. Canan ÖZGEN
Dean, Graduate School of **Natural and Applied Sciences** _____

Prof. Dr. Zuhâl KÜÇÜKYAVUZ
Head of Department, **Micro and Nano Technology** _____

Dr. Burcu AKATA KURÇ
Supervisor, **Department of Micro and Nano Tech., METU** _____

Prof. Dr. Raşit TURAN
Co-Supervisor **Department of Physics, METU** _____

Examining Committee Members:

Prof. Dr. Macit ÖZENBAŞ
Department of Metallurgical and Material Eng., METU _____

Dr. Burcu AKATA KURÇ
Department of Micro and Nano Tecnology, METU _____

Prof. Dr. Raşit TURAN
Department of Physics, METU _____

Prof. Dr. Hayrettin YÜCEL
Department of Chemical Eng., METU _____

Asst. Prof. Can ÖZEN
Department of Biotechnology, METU _____

Date: 04.05.2010

I hereby declare that all information in this document has been obtained and presented in accordance with academic rules and ethical conduct. I also declare that, as required by these rules and conduct, I have fully cited and referenced all material and results that are not original to this work.

Name, Last name: Seçkin ÖZTÜRK

Signature :

ABSTRACT

IMMOBILIZATION OF ZEOLITE CRYSTALS ON SOLID SUBSTRATES FOR BIOSENSOR APPLICATIONS

ÖZTÜRK, Seçkin

M.Sc., Department of Micro and Nano Technology

Supervisor: Dr. Burcu AKATA KURÇ

Co-Supervisor: Prof.Dr. Raşit TURAN

May 2010, 76 pages

Electrochemical biosensors are cost effective, fast and portable devices, which can determine the existence and amounts of chemicals in a specific medium. These devices have many potential applications in many fields such as determination of diseases, process and product control, environmental monitoring, and drug research. To realize these potentials of the devices, many studies are being carried out to increase their sensitivity, selectivity and long term stabilities. Surface modification studies with various types of particles (metal nano particles, carbon nano tubes etc.) can be count among these studies.

Although zeolites and zeo-type materials are investigated for many years, they still hold interest on them due to their capabilities. By means of their chemical resistances, large surface areas, tailorable surface properties, and porous structures they can be applied in many applicational fields. In some recent studies, these properties are intended to be used in the field of biosensors.

The purpose of the current study was to investigate the effect of zeolite nanoparticles on electrochemical biosensor performances. Firstly, several different procedures were investigated in order to find the best and optimum methodology

to attach previously synthesized zeolites on Si wafer substrates for the first time. For this purpose, the ultrasonication, spin coating and direct attachment methods were used and their efficiencies were compared. Perfectly oriented, fully covering, zeolite monolayers are produced by direct attachment method. Successively produced zeolite thin films were then patterned with the help of Electron Beam Lithography technique to show the compatibility of coating methods to the CMOS technology. Combination of Direct Attachment and EBL techniques resulted well controlled zeolite monolayer patterns.

Then zeolite modified electrochemical biosensors were tested for their performances. With these experiments it was intended to improve the selectivity, sensitivity and storage stabilities of standard electrochemical biosensors. Experiments, conducted with different types of zeolites, showed that zeolites have various effects on the performances of electrochemical biosensors. Amperometric biosensor response magnitudes have been doubled with the addition of Silicalites. Faster conductometric electrode responses were achieved with enzyme immobilization on zeolite film technique. Also it is seen that Beta type zeolites modified through different ion exchange procedures, resulted different responses in IS-FET measurements.

Keywords: Zeolite, Electron Beam Lithography, Biosensor, Thin film

ÖZ

BİYOSENSÖR UYGULMALARI İÇİN KATI YÜZEYLERE ZEOLİT KRİSTALLERİNİN TUTTURULMASI

ÖZTÜRK, Seçkin

Yüksek Lisans, Mikro ve Nano Teknoloji Bölümü

Tez Yöneticisi: Dr. Burcu AKATA KURÇ

Ortak Tez Yöneticisi: Prof.Dr. Raşit TURAN

Mayıs 2010, 76 sayfa

Elektrokimyasal Biyosensörler, belirli bir ortamda bulunan kimyasalların varlıklarını ve miktarlarını tesbit etmekte kullanılan hızlı, ucuz ve taşınabilir cihazlardır. Bu cihazların hastalık tesbiti, proses ve ürün kontrolü, çevresel izleme, ilaç araştırmaları gibi birçok alanda kullanılma potansiyeli vardır. Bu potansiyelleri hayata geçirmek için cihaz hassasiyetlerinin, seçiciliklerinin, raf ömürlerinin ve çalışma kararlılıklarının artırılmasına yönelik birçok çalışma yürütülmektedir. Bu çalışmalar arasında yüzeylerin çeşitli partiküllerle (metal nano partikül, karbon nanotüp vb.) modifiye edilmesi de vardır.

Zeolitler ve zeolit türü malzemeler çok uzun yıllardan beri araştırılmalarına rağmen sahip oldukları özellikler sayesinde halen yoğun bir araştırma konusudur. Kimyasal dayanıklılıkları, büyük yüzey alanları, değiştirilebilir yüzey özellikleri, gözenekli yapıları ve benzer başka özellikleri sayesinde birçok konuda uygulama alanı bulabilmektedirler. Yakın zamanda yapılan bazı çalışmalarda zeolitlerin bu özelliklerinden biyosensör konusunda da faydalanılması amaçlanmıştır.

Bu çalışmanın amacı zeolit nanopartiküllerinin elektrokimyasal biyosensör performansına etkisini araştırmaktır. İlk olarak, önceden sentezlenmiş zeolitlerin Si tabaka üzerine tutturmanın en iyi ve uygun yöntemini bulmak için birçok farklı yöntem ilk kez incelenmiştir. Bunun için ultrasonik kaplama, döndürerek kaplama ve doğrudan tutturma gibi yöntemler uygulanmıştır. Tam olarak düzenli, yüzeyi tam kaplayan, tek katmanlı zeolit filmler doğrudan tutturma yöntemi ile üretildi. Devamında, kaplama yöntemlerinin CMOS teknolojisine uyumluluğunu göstermek için, başarıyla üretilmiş zeolit filmler, Elektron Demet Litografisi tekniğiyle desenlenmiştir. Elektron Demet litografisi ve doğrudan tutturma yöntemlerinin birleşimi sonucunda, iyi kontrol edilebilen, desenlenmiş zeolit tek katman filmler elde edildi.

Daha sonradan zeolitle modifiye edilmiş elektrokimyasal biyosensörlerin performansları test edilmiştir. Bu şekilde Elektrokimyasal biyosensörlerin seçicilik, hassasiyet ve kararlılık özelliklerinin geliştirilmesi amaçlanmıştır. Farklı zeolit türleriyle gerçekleştirilmiş deneyler, zeolitlerin elektro kimyasal biyosensör performansı üzerinde etkisi olduğunu göstermiştir. Amperometric biyosensör tepkileri Silicalite eklenmesi ile iki katına çıkarıldı. Zeolit film üzerine enzim tutturma yöntemiyle daha hızlı conductometric sensör tepkileri elde edildi. Ayrıca farklı ion değiştirme yöntemleriyle modifiye edilmiş Beta tipi zeolitlerin IS-FET tepkilerinde değişikliğe yol açtığı gözlemlendi.

Anahtar Kelimeler: Zeolit, Elektron Demet Litografisi, Biyosensör, İnce Film.

to my lovely family...

ACKNOWLEDGEMENTS

I would like to thank to my supervisor Dr. Burcu AKATA KURÇ for providing any opportunity needed to carry out this work. Her encouragement, perceptiveness and friendship played a crucial role in conclusion of this study. Also I would like to thank to my co-supervisor Prof. Dr. Raşit TURAN for supporting this work with his laboratory facilities and scientific ideas.

I would also like to thank to METU Central Laboratory, for enabling its wide facilities anytime needed in this work and specially Prof. Dr. Hayrettin YÜCEL for allowing me to conduct this study.

Also, I would like to thank to Kübra KAMIŞOĞLU for providing LTA zeolites, Tatiana GORIUSHKINA and Alexander SOLDATKIN for their contributions to electrochemical biosensor measurements.

I am grateful to my research group partners Berna OZANSOY, Esin SOY, Kaan KİRDECİLER and Sezin GALİOĞLU for their friendliness and support during this work. I would like to extend my thanks through my colleague and friends, Sedat CANLI, İlker YILDIZ, Özgür ERİŞEN, Leyla MOLU, Eda Ayşe AKSOY, Elif TARHAN BOR, Levent YILDIZ, Uğur ÖZGÜRGİL and many others for their friendship and motivation.

This study is partially funded by European Union Project NanobioSens and partially supported by to Scientific and Technological Research Council of Turkey (TÜBİTAK) and these grants are gratefully acknowledged.

Finally, it is my pleasure to express my gratitude towards my wife Aycan BAKTİR ÖZTÜRK, who has been with me for years with patience.

TABLE OF CONTENTS

ABSTRACT	iv
ÖZ	vi
ACKNOWLEDGEMENTS	ix
TABLE OF CONTENTS.....	xx
LIST OF FIGURES	xiii
LIST OF TABLES	xvii
LIST OF ABBREVIATIONS	xviii
CHAPTERS	
1. INTRODUCTION	1
1.1. Principles of Electrochemical Bio-Sensors	3
1.1.1. Conductometric Biosensors	3
1.1.1.1 Advantages and Disadvantages.....	4
1.1.1.2 Measurement Set-Up:.....	5
1.1.2 Amperometric Biosensors	6
1.1.2.1 Advantages and Disadvantages.....	7

1.1.2.2 Measurement Setup.....	8
1.1.3. ISFET & ENFET Biosensors	9
1.1.3.1 Advantages and Disadvantages.....	10
1.1.3.2 Measurement Setup.....	10
1.2 Effect of Surface properties on Bio-Sensor performance	12
1.3 Zeolites for Biosensor Applications.....	13
2. LITERATURE REVIEW.....	14
2.1. Enzyme Immobilization on Zeolite Surfaces	14
2.2. Oriented assembly of zeolites and Micro Patterning	16
3. EXPERIMENTAL	21
3.1. Zeolite Immobilization and Patterning.....	21
3.1.1. Zeolite Immobilization.....	21
3.1.1.1. Spin Coating.....	21
3.1.1.2. Ultrasonic Agitation	21
3.1.1.3. Direct Attachment	22
3.1.2. Zeolite Patterning	22
3.1.3. Characterization	23
3.2. Biosensor Measurements	23
3.2.1. Conductometric measurements	26
3.2.2. Amperometric measurements.....	28
3.2.2. ISFET measurements	31

4. RESULTS AND DISCUSSIONS	32
4.1. Zeolite Immobilization and Patterning.....	32
4.1.1. Zeolite Immobilization.....	32
4.1.1.1. Spin Coating.....	33
4.1.1.2. Ultrasonic Agitation.....	34
4.1.1.3. Direct Attachment.....	35
4.1.2. Zeolite Patterning.....	40
4.1.2.2 Pattern Formation by using Direct Attachment Method.....	43
4.1.2.3 Formation of Line Patterns and Controlled Thicknesses of Zeolite A Nanocrystals using Direct Attachment Method.....	45
4.2. Biosensor Measurement Results	49
4.2.1. Conductometric measurement results	50
4.2.1.1 Effect of zeolite loading into bioselective membranes	50
4.2.1.2 Results of zeolite film coated electrodes.....	52
4.2.2. Amperometric measurements results	54
4.2.3. ISFET measurement results	61
4.2.3.1. Effect of zeolite loading on pH sensitivity.....	61
4.2.3.2. Zeolite added Enzyme Membrane Results:.....	62
5. CONCLUSIONS.....	65
REFERENCES.....	67
APPENDIX A Table of Zeolite samples	72

LIST OF FIGURES

FIGURES

Figure 1.1: Scheme of the Conductometric measurement system.....	5
Figure 1.2: Equivalent circuit diagram of the sensor-solution system.....	5
Figure 1.3: Schematic representation of two different measurement setups. A) two-electrode system. B) three – electrode system.....	8
Figure 1.4: Schematic representation of Field Effect Transistor (A) and an IS-FET device.....	9
Figure 1.5: Schematic representation of IS-FET readout circuit.....	11
Figure 3.1: Schematic representation of the fabrication of zeolite nanocrystals on Si wafer.....	23
Figure 4.1: SEM images of spin coated samples. 1% zeolite concentration (A) and 10% zeolite concentration (B) in IPA.....	33
Figure 4.2: SEM low magnification (A) and High magnification (B) images of ultrasonic agitation samples.....	35
Figure 4.3: The SEM image showing the zeolites A attachment results obtained upon application of direct attachment method on Si wafer substrates.....	33

Figure 4.4: SEM images of zeolite immobilization experiments. a) Spin Coating b) Ultrasound aided agitation c) Direct attachment.....	37
Figure 4.5: X-ray powder diffraction patterns of randomly oriented zeolite A nanocrystal powder (a), Si wafer (b), and uniformly oriented zeolite A nanocrystal monolayer on Si wafer after the application of direct attachment method (c).....	39
Figure 4.6: SEM image of the patterns generated by the combination of EBL and Spin Coating.	41
Figure 4.7: The SEM image showing the loss of all patterns formed on the Si wafer substrate upon the application of spin coating zeolites A crystals. The dashed lines show where the patterns were formed by EB lithography...	42
Figure 4.8: SEM image of zeolite micro-patterns on Si wafer obtained upon using direct attachment method.....	43
Figure 4.9: SEM images of monolayers of zeolite A nanocrystal stripe patterns with different line widths on Si wafer (a), and high magnification images of zeolite stripes formed of single (b) and double zeolite rows (c).....	46
Figure 4.10: AFM images of ca. 400 and 850 nm PMMA coated and developed Si wafers (a and c); SEM image of zeolite monolayer on the developed Si wafer with 400 nm (b) and SEM image of zeolite double layer on the developed Si wafer with 850 nm (d) PMMA resist.....	48
Figure 4.11: Schematic Representation of standard membranes and zeolite added membranes.....	50
Figure 4.12: Normalized responses of conductometric urease biosensors to 8 mM urea without and with different types of zeolites. Na ⁺ -Beta-30 (1), NH ₄ ⁺ -Beta 30 (2), H ⁺ -Beta 30 (3) , Na ⁺ -Beta 50(4), NH ₄ ⁺ -Beta 50(5), H ⁺ -Beta 50 (6).....	51

Figure 4.13: Schematic representation of zeolite film coated electrodes.....	52
Figure 4.14: Calibration curves for urea determination for conductometric biosensors based on urease using enzyme membrane on zeolite film (1), enzyme on zeolite film (2) and standard enzyme membrane (3).....	52
Figure 4.15: Typical response curves of conductometric biosensor based on urease using enzyme membrane on zeolite film (1), enzyme on zeolite film (2) and standard enzyme membrane (3) for 0,5 mM urea	54
Figure 4.16: Calibration curves of amperometric biosensors based on platinum printed SensLab electrode with GOD with Silicalite-1 immobilized in PEDT (1) and in GA (3) and GOD with Silicalite-2 immobilized in PEDT (2) and in GA (4). Measuring conditions: 20 mM phosphate buffer, pH 7.2, at potential of +200 mV versus intrinsic reference electrode.....	55
Figure 4.17: Calibration curves of glucose amperometric biosensors based on GOD without zeolite (4) and GOD with zeolites Silicalite-1 (1), Silicalite-2 (2), NH ₄ -Beta-25 (3), Na-Beta (5), H-Beta-300 (6), H-Beta-150 (7), immobilized in PEDT. Measuring conditions: 20 mM phosphate buffer, pH 7.2, at a potential of +200 mV versus intrinsic reference electrode.....	56
Figure 4.18: Responses of glucose amperometric biosensors to ethanol based on GOD without zeolite (4) and GOD with zeolites Silicalite-1(1), Silicalite-2 (2), NH ₄ -Beta-25 (3), Na-Beta (5), H-Beta-300 (6), H-Beta-150 (7), immobilized in PEDT. Measuring conditions: 20 mM phosphate buffer, pH 7.2, at a potential of +200 mV versus intrinsic reference electrode.....	57
Figure 4.19: Response to pH change for different zeolites. -Beta-30 (1), NH ₄ -Beta 30 (2), H ⁺ -Beta 30 (3) , Na ⁺ -Beta 50(4), NH ₄ -Beta 50(5), H ⁺ -Beta 50 (6).....	62

Figure 4.20: ISFET responses to urea using different zeolites. Na-Beta-30 (1), NH₄⁺-Beta 30 (2), H⁺-Beta 30 (3), Na⁺-Beta 50(4), NH₄⁺-Beta 50 (5), H⁺-Beta 50 (6)..... **63**

Figure 4.21: Repeatability experiment results for standard and zeolite added membranes..... **64**

LIST OF TABLES

TABLES

Table 3.1: List of zeolite samples and their synthesis procedures.....	25
Table 4.1: Summary of zeolite modified amperometric biosensor results.....	59

LIST OF ABBREVIATIONS

PMMA Poly(Methyl metacrlate)

EBL Electron Beam Lithography

XRD X-Ray Diffraction

ISFET Ion Sensitive Field Effect Transistor

LBL Layer by Layer

GA Glutaraldehyde

SEM Scanning Electron Microscope

AFM Atomic Force Microscope

PBS Phosphate buffer Solution

EN-FET Enzyme - Field Effect Transistor

CHAPTER 1

INTRODUCTION

Biosensors are highly selective, fast responding and inexpensive tools for biomolecule detection. With the increasing importance of biomolecule detection, they are becoming indispensable elements of this field. On the other hand, to fulfill the demands coming from this field, they need to be developed further.

Bio-molecules are both the indicators of human health status and the measurable quantities of the human activity products. One can easily monitor the health status of a person by measuring the level of the bio-molecules in the person's body fluids. Disorders, diseases, infections, intoxications leave some diagnosable tracks in the body fluids. Also agricultural activities and products are needed to be investigated by means of bio-molecules to guarantee the food quality and healthiness. Moreover, industrial products, mid-products and by-products are subjects of bio-molecule measurements. By quantifying the bio-molecule contents of these materials it can be possible to measure the environmental effects of the industrial activity, process efficiency and product quality. As the needs of bio-molecule detection increases, it became more important to find easy, fast and inexpensive methods.

There are tens of bio-molecule detection techniques which range from highly dedicated, expensive and slow systems (i.e., mass spectrometers, chromatography systems, Nuclear Magnetic Resonators, etc.) to simple and inexpensive ones like biosensors.

Biosensors can be classified into five main groups, which are Piezoelectric, Calorimetric, Photometric, Optical and Electrochemical sensors. Piezoelectric biosensors are resonating crystals which has a bio-functionalized surface. The resonance frequencies of the crystals can be changed with the mass of the bonded analytes. The observed, “shifts in the resonance frequency” can be detected and converted into electrical signals with the help of Lock-In Amplifiers.

Many enzyme-catalysed reactions are exothermic, generating heat which may be used as a basis for measuring the rate of reaction and, hence, the analyte concentration in calorimetric biosensors. The temperature changes are usually determined by means of thermistors and can be registered as analyte concentration.

In the case of photometric biosensors, surface plasmon resonance phenomenon is utilized. Incoming laser beam generates plasmonic waves on bio-recognition molecule coated thin metallic layers. In the presence of target molecule, refractive index of the surrounding changes; that gives rise to a recognizable change in plasmonic signals. These optical signals should be converted into electrical signals to be processed.

Optical biosensors are uses the change of other optical properties to sense the presence of the biomolecules. Presence and the amount of the target molecule changes the absorption, reflection properties of the medium or the florescence properties of the sensitive surfaces which rise to a color change of the biosensor.

Electrochemical biosensors are sensors which are sensitive to chemical changes in their environment. These chemical changes are produced by the bio-activity of bio-recognition elements which are bonded on their surfaces. Details of the electrochemical biosensor principles will be given in the following section.

1.1. Principles of Electrochemical Bio-Sensors

Measurement principles of electrochemical biosensors are simple when compared with other types of biosensors. Their transducers produce electrical signals which do not need to be converted. This property makes electrochemical biosensors small, inexpensive and suitable for batch production processes. Electrochemical biosensors are divided into three categories: Amperometric, Conductometric and Potentiometric. Working principles of conductometric biosensors, amperometric biosensors and EN-FETs which are sub type of Potentiometric biosensors will be given in this section.

1.1.1. Conductometric Biosensors

Conductometric biosensors simply measure the conductivity of the solution as can be understood from the name of the method. Almost every solution contains ions (positive charged cations and negative charged anions). If two metal wires are dipped into a solution and a potential is applied to these metals, an electric field is induced and the ions move along the electric field (cations to negative side and anions to positive side). The motion of the ions in the solution leads to a measurable current. According to the well known Ohm's law; conductivity of the solution can be calculated.

$$S = I / V \quad (1.1)$$

Where S is the conductivity, V and I are the applied potential and the induced current respectively. Specific conductivity can be calculated with the following equation.

$$X = (S L)/A \quad (1.2)$$

Where X is the specific conductivity, L is the distance between the immersed metals and A is the area of the metal solution interface. X is the main interest of this type of measurements. If we neglect the other parameters and represent them as one constant C , X can be explained as:

$$X = C \sum(u_i c_i) \quad (1.3)$$

Where u_i is the mobility of an ion, c_i is the concentration of an ion and C is the representation of the hidden parameters. As the enzymatic reaction occurs, these two parameters change. Some ions can be produced or consumed as a result of the reaction or the viscosity of the environment changes. By this way variation of X can be measured as an indicator of enzymatic reaction.

1.1.1.1 Advantages and Disadvantages

Conductometric biosensors can be fabricated easily with low costs because of their simple structure. Also due to their simple principles they can be used with many (almost all) types of enzymes, for many types of applications.

These devices, contrary to the other types of sensors, do not measure the enzymatic reaction, but the resultant conductivity change. Background conductivity of the solution (without the existence of enzyme) is also measured at the same time which can be influenced by some other factors. Because of that, these devices are known with their low selectivity.

1.1.1.2 Measurement Set-Up:

Measurement can be done with a simple set-up (Figure 1.1 and Figure 1.2). A function generator which can supply frequencies up to 100 kHz and currents up to a few mA may be enough as the alternating power supply. Lock-in Amplifier differentiates two signals coming from two electrode pairs (working and reference), amplifies and digitalizes to be read by the computer. Acquired data can be stored and analyzed by the computer or data plotter.

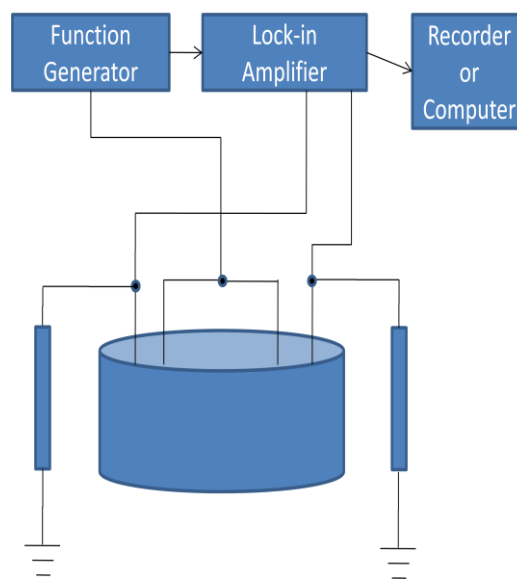


Figure 1.1: Scheme of the Conductometric measurement system.

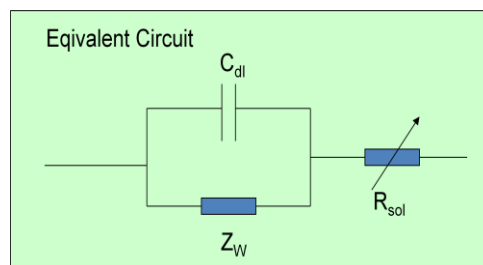


Figure 1.2: Equivalent circuit diagram of the sensor-solution system.

A similar measurement system can be set up also with Impedance analyzers. But this time the name of the method slightly changes. The word “**Impedometry**” should be used instead of conductometry. By impedometry; one can identify not only the conductance/resistance of the system but also the double layer capacitances, ion mobilities etc. Most of the Impedance analyzers do not have the ability to measure two electrodes at the same time. With the available systems we can only do single (without reference) electrode measurements.

1.1.2 Amperometric Biosensors

Amperometric biosensors are the first type of biosensors, which are developed and investigated. Today, most of the commercially available biosensors are based on amperometry.

This method has a more complicated mechanism when compared with the other techniques. This technique simply measures the electron transfer between the electrodes and the solution, which is induced by the electrochemical reactions. If a small potential is applied to the electrodes, an electric current occurs due to the motion of the charged particles. If the applied potential exceeds a specific value, Red/Ox reactions start inducing an extra current through the electrode – solution interface.

Through our aspect, Red/Ox reactions can be summarized as charge transfer reactions. Oxidized particles consume electrons while they are being reduced and reduced particles generate electrons while they are being oxidized. Electron transfer reaction is as follows.



Where; z is the number of electrons that is required for one Red/Ox reaction.

The total current of the system can be used to determine the reaction yield on the electrode surface. Total current of the system is the sum of the Cathode and Anode currents.

$$I = I_c + I_a \quad (1.5)$$

$$I_c = zFk_c C_{Ox} \quad (1.6)$$

$$I_a = -zFk_a C_{Red} \quad (1.7)$$

Where z is charge, F is Faraday constant, C_{Ox} and C_{Red} are concentrations of Ox and Red particles respectively. k_c and k_a are electrode constants which describe the reaction rates and functions of the applied potential. As can be seen from the equations, substrate concentrations are determining factor for the total current of the system and total current can be used to measure the substrate concentrations.

1.1.2.1 Advantages and Disadvantages

These types of sensors are well known and widely commercialized devices. The most advantageous point of this technique is its selectivity. The sensors are able to measure directly the specific reaction and its resultant current where all the other methods measure the resultant changes of the environment. This property not only enhances the selectivity but also limits the enzyme types and application fields. Only the reducing and oxidizing enzymes can be used and their specific substrates can be measured with this technique.

1.1.2.2 Measurement Setup

Measurements can be done with a voltage supply, a voltmeter and a nanoammeter. Applied potential is swept between certain values while the potential drop on the solution and the current through the solution is recorded. In Figure 1.3 the scheme of two simple measurement setups can be seen.

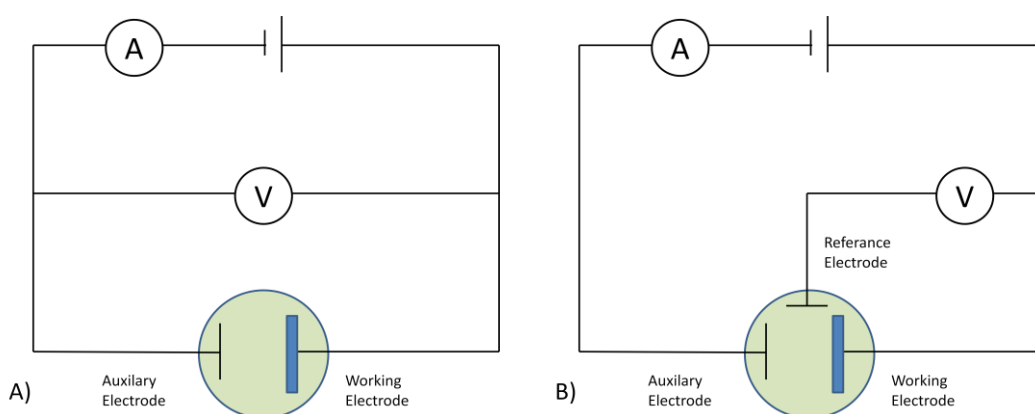


Figure 1.3: Schematic representation of two different measurement setups. A) two-electrode system. B) three – electrode system.

There are two measurement techniques. In the two electrode system, same nodes are used for both supplying voltage and measuring potential drop. Because of this, only the total potential drop on the solution is measured instead of the net potential drop on the working electrode. To get rid of this problem (to eliminate the potential drop on the auxiliary electrode) a third electrode can be introduced. In this case, potential drop is measured through the reference electrode and net potential drop on working electrode can be measured.

In most of the laboratories, dedicated and relatively inexpensive amperometry measurement equipments are used for measurements. (Voltalab, Palmsens)

1.1.3. ISFET & ENFET Biosensors

ISFETs are semiconductor devices which are based on the principles of Field Effect Transistors (FET). Basically, FET devices are composed of two serially but reverse connected p-n junctions (Figure 1.4). This structure generates a “not passable gate” for neither direction. This structure is isolated with an insulator layer which is named as “Gate Insulator”. As a net charge accumulates on the surface of the insulator, opposite charges in the device populates the region near the insulator due to the induced electric field. This populated region then behaves like a “channel” through this ‘not passable gate’ which allows a current pass through the device. The amount of the current depends on the width of the channel which is defined by the accumulated charge on the insulator.

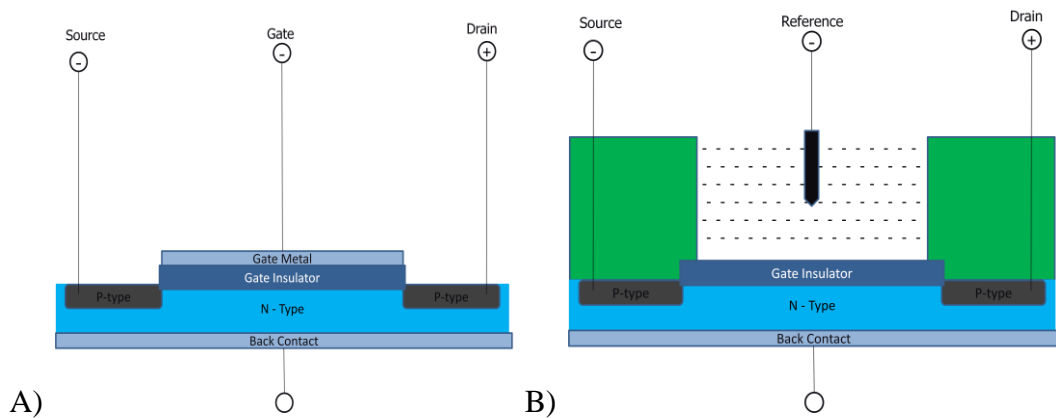


Figure 1.4: Schematic representation of Field Effect Transistor (A) and an IS-FET device.

ISFET devices function based on the above mentioned principles. Gate insulator, which is facing the solution, is used as the sensitive region of the device. The surface charge of the gate insulator is affected by the pH of the solution. ISFETs with a bare insulator surface behave like pH sensitive devices. If the surfaces of the ISFETs are functionalized by the bio-active membranes, bio sensitive devices can be made. Enzyme activated ISFETs are named as ENFETs. ENFETs measures resultant pH changes of enzymatic reactions.

1.1.3.1 Advantages and Disadvantages

ISFETs are products of microelectronic technology, which makes them fully compatible with microelectronics. This property allows them to be easily and cost effectively produced in arrays with their read-out circuits on a small area. On the other hand their applications are limited to some of the enzymes. Only the enzymes which induce pH changes can be used with ENFETs.

1.1.3.2 Measurement Setup

Although, dedicated four point measurements systems are available, generally custom made, simple “drain voltage follower” circuits are enough for ISFET measurements. A “saturated calomel” reference electrode is used to maintain the potential between the back contact of the ISFET and the solution. The current between drain and source is measured as the indicator of the pH level around the surface of the gate insulator.

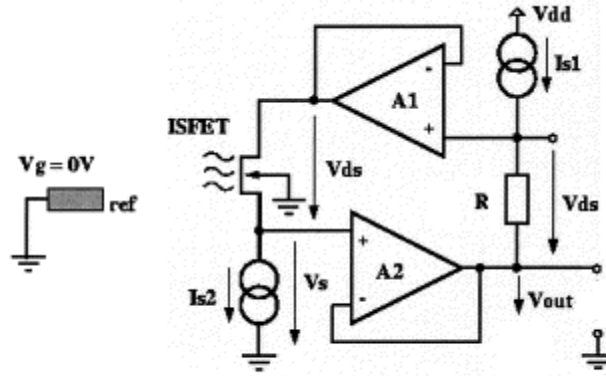


Figure 1.5: Schematic representation of IS-FET readout circuit.

The drain current of the ISFET is driven by the current sink I_{s2} and the drain-source voltage V_{ds} is fixed by the current source I_{s1} and resistor R . A change in ion activity will lead to a change of the common mode level of V_{ds} with respect to ground. ISFET works in the linear region. When $V_g=0V$ and $V_{gs}=-V_s=-V_{out}$, the expression for V_{out} is derived as:

$$V_{out} = -V_{th} - \frac{I_{s2}}{\beta \cdot I_{s1} \cdot R} - \frac{I_{s1} \cdot R}{2} \quad (1.8)$$

$$V_{th} = (R_g \cdot T/F) \cdot \log(H^+) \quad (1.9)$$

Where, β is the gain coefficient, R_g is the gas constant, T is the absolute temperature (K), F is the Sensors Faraday constant and H^+ is the hydrogen-ion concentration. When R , I_{s1} and I_{s2} are constants, V_{out} is proportional to a change in ion activity represented by the threshold voltage V_{th} of the ISFET sensor.

1.2 Effect of Surface properties on Bio-Sensor performance

Almost all the performance parameters (sensitivity, selectivity, long term stability) of the electrochemical biosensors are defined by the surface properties of the sensors. All the enzymatic reactions, which can be detected, take place on the sensor surface.

Biocompatibility of the surfaces is one of the most important properties of the sensor surfaces. Enzyme activity should not be inhibited by the surface and also enzymes should not degrade due to the surface properties. These are important for the sake of high sensitivity and long term stability.

Another important parameter for the surface is conductivity, especially for amperometry and conductometry. Conductance of the surface should not be the limiting factor for the electrochemical signals passing through surface to the transducer. Sensitivity of the sensors can be affected with the conductance of the surface.

Number of binding sites also has effects on sensitivity. Number of binding sites defines the number of hosted enzyme and reaction rate in most cases. Signal amplitude depends on the number of binding sites.

For the sake of selectivity, surfaces should not react with non-specific chemicals. Otherwise signals of the enzymatic reaction of the target molecule can be mixed with the non-specific signal which leads to a low selectivity.

To improve above mentioned properties of sensor surfaces many surface modification methods are being investigated in the literature. These methods can be summarized as; polymeric membrane coating, metallic nano particle immobilization, ceramic nano particle immobilization, etc.

1.3 Zeolites for Biosensor Applications

Zeolites are porous, chemically stable, biocompatible materials which has high number of surface groups. Regarding these properties zeolites are seen to be good candidates as enzyme hosts for biosensor applications. Their surfaces can be populated with enzymes by means of their high number of surface groups and kept active by means of chemical stability and bio compatibility. Also pores of the zeolites may isolate enzymes and this can protect enzymes from hazardous environmental effects. Moreover pores can behave like selective membranes for products or interfering substances of appropriate sizes, which can improve the selectivity of the sensors.

In the current thesis study, it was aimed to obtain improved electrochemical biosensor performances by the incorporation of zeolites into each biosensor system. For this particular purpose, different zeolite immobilization techniques on Si wafer substrates were deeply studied. The obtained results and methodologies were studied to understand the effect of modifying the electrode surfaces by zeolite crystals on the performance of biosensors. Results obtained from different trials accomplished using different bio sensors are further discussed.

CHAPTER 2

LITERATURE REVIEW

The studies related with using zeolites and zeo-type materials as alternative materials in biosensor applications are getting more attention every year. Although, zeolites can be considered as promising candidates for enzyme immobilization studies, the fact that they are found in powder form limits the research done for integrating zeolites with biosensor systems. Accordingly, it is believed that not only using zeolites in biosensor applications is a major challenge, but also assembly of these crystals onto different substrates is something that needs to be achieved before taking biosensor measurements. Thus, the related literature work is also divided into these two sections:

2.1. Enzyme Immobilization on Zeolite Surfaces

One of the main interest into improved biosensor performances is due to the importance of obtaining long-term stability of enzyme electrodes, which has been a common research interest since the development of the first glucose biosensor by Clark and Lyons in 1962 [1]. Although many improvements have been reported from that date, there is still a significant need for new approaches in this

field, because many enzyme electrodes are still suffering from long term stability and performances which prevents them being commercialized. In general, the conventional techniques for enzyme immobilization include covalent attachment of enzymes onto the electrode surfaces [2-4], entrapment of enzymes into polymers [5, 6], and cross-linking enzymes with in bovine serum albumin-glutaraldehyde [7] or regenerated silk fibroin [8] immobilization matrix, etc.

Since 1970s, some inorganic materials, such as silica, alumina, glass, and zeolites, have been proven to be good candidates to be enzyme immobilization matrices [9-15]. Zeolites can be considered as being one of the most promising type of inorganic materials due to their tailorable surface and structural properties, controllable pore sizes and morphologies, and high specific surface areas in addition to other properties existing in the above mentioned inorganic materials, such as good mechanical, thermal, and chemical stability. Moreover ion-exchange and catalytic properties attract considerable interest into zeolites [16]. Regarding these properties of zeolites, several different studies were reported in the literature investigating the enzyme immobilization on zeolites and zeo-type materials. Among these studies, only a few of them are related with the investigation of the electrochemical biosensors modified with zeolites.

Mukhopadhyay et al. reported an enzyme immobilization technique where Na-Y particles are used as solid supports of enzymes [17]. Synthesized and AP-TES functionalized Na-Y particles were first stirred for 12 hours in colloidal nanogold particle solution to produce nanogold modified zeolite particles. These particles were then introduced into the pepsin solution and were stirred 1 hour. The authors' objective was to obtain reusable properties. Accordingly, it was shown that upon using Na-Y zeolites, the purpose was achieved. Produced Pepsin- Nano Gold -Zeolite conjugates were observed to possess good activities and reusable properties.

Ma et al. reported another enzyme immobilization technique where pores of zeo-type material were utilized [18]. Synthesized and calcined mesoporous MCM-41 powder was mixed and stirred in lipase solution. Activity of the calcined and

enzyme modified MCM-41 was compared with the activity of non calcined and enzyme modified ones. The calcined MCM-41 presented better activity and reasonably good reusability. This showed that lipase molecules were immobilized into the pores of MCM-41 particles.

The effect of surface groups and pore sizes were also investigated in another study by Xing et al [19]. The zeolites used for that particular purpose were HY, NaY, NH₄Y, and dealuminated zeolite Y (HDAY, HNH₄DAY) and activities of zeolite incorporated enzyme systems and free enzymes were compared using these zeolites. Accordingly, performance of the HY incorporated enzymes was reported to be the highest and Dealuminized Y zeolites showed the worst performances. This study also proved that the structural and the surface properties have differentiable effects on the enzymatic activities.

Dealuminated zeolite Y (DAY) was also used by Deng et al. for modifying the electrodes [20]. One of the first zeolite modified electrochemical biosensor was introduced in this study. Platinum substrates were coated with Poly-vinylalcohol (PVA) solution (PVA-Pt) or DAY added PVA solution (DAY-Pt) and dried. Prepared substrates were immersed into glucosoxidase solutions for 24 hours for the enzymes to be adsorbed onto the surfaces. Afterwards, washed substrates were subjected to amperometric measurements. DAY modified electrodes were shown to withstand drastically high pHs, temperatures, and possess longtime storage stabilities. With these results authors claimed that, enzymes can be protected from environmental effects by putting them into zeolite pores.

2.2. Oriented assembly of zeolites and Micro Patterning

Zeolites are materials which can be used in many industrial and technological applications as microporous sieves for molecular separation [21, 22], low-dielectric materials [23–25], thin film catalysts [26, 27], size-selective sensing devices (1)[34], and as modified electrodes [29–32]. Moreover these materials can be used as advanced materials in the semiconductor technology [21-34]. On the

other hand zeolites are in powder form and they need to be attached on solid substrates. Because of that, organization of zeolites on various substrates as mono or multi layers is of great interest with various respects [36–45]. Organized zeolite layers are necessary but not enough for some applications. Patterning [46, 47] of these layers is required to be able to produce devices especially in sensor applications and semiconductor technologies.

In general, two main approaches can be found in the literature to form zeolite mono/multilayers on solid substrates. These are growing zeolite crystals on substrates and attaching pre-synthesized zeolite crystals onto substrates.

Growth on the surface approach can be divided into three main steps. First zeolite crystals, which will be used as seeds, are synthesized with conventional techniques. Synthesized seed crystals are deposited onto substrates with spin coating or dip coating methods. Afterwards seeded samples are dipped into zeolite synthesis solutions for a period of time until desired film is achieved. With this approach it is possible to achieve strongly bonded fully covered zeolite thin films. On the other hand this approach requires exposure to strong chemicals during the secondary growth step which limits its applications.

Work of Jacob et al can be given as an example to this approach [48]. Clean silicon substrates are spin coated with pre-synthesized Beta zeolite suspensions. Seeded substrates are calcined to prevent them falling during the secondary growth prior to the immersion into zeolite synthesis solution. After a 9 day of secondary growth period successive zeolite films are achieved.

Second approach includes many methods like spin coating, dip coating, ultrasonic agitation and direct attachment. This approach does not necessitate exposure to strong chemicals which makes it advantageous for many applications.

Dip-coating was conducted by immersing substrates into the zeolite suspension and removing it at a certain speed. Substrates are then dried in ambient conditions. As the solvent evaporates a zeolite monolayer is remained on the surface of the substrates. In this technique, multiple dip-coatings were often needed to achieve

fully covered zeolite films on substrate surfaces. Tsapatsis et al. [49] applied subsequent dip-coatings and drying procedures up to 5 times to fabricate fully covered silicalite-1 layer. Besides, Takahashi et al. [44] immersed substrates into zeolite suspensions at a tilt angle of 45°. As the result fully covered and (h00)-oriented LTA-type zeolite layers was formed. Bein et al. [50] utilized the spin-coating technique by dripping zeolite suspensions on rotating substrates like Si wafers and Gold. Multilayer films of *b*-oriented ZSM-5 crystals (15 and 30 nm) were formed where the thickness of the film can be controlled by the concentration of the zeolite suspension.

Another similar deposition technique was reported Jung et al. [51] for assembly of zeolite crystals on solid substrates. A glass substrate was covered with zeolite suspension (0.2 wt.% ZSM-5) and dried at ~100° C. As the solvent evaporated, zeolite particles are attached to the hydroxyl groups on the glass surface. At the end, a monolayer of closely packed zeolite film was remained on the glass surface. It was supposed that this method can be used to produce high quality zeolite membranes because of its being simple and applicable to variety of zeolite types.

Yoon et al. [42], introduced ultrasonication method as an alternative way of forming zeolite films. Functional group bearing substrates are immersed in zeolite suspensions in toluene and sonicated for long durations. As a result well organized and closely packed zeolite monolayers are achieved with a high degree of coverage (>90%).

Yoon et al. [52] also reported totally solvent free monolayer formation method. Zeolite powder is rubbed onto substrate surface utilizing a latex glove bearing finger. After a certain time of rubbing, fully covered, densely packed, well organized zeolite monolayers are formed on substrates. In his report Yoon claimed that this method is a facile method for zeo-type materials which are bigger than 500 nm.

If zeolite films can be patterned on solid substrates, applications of zeolite films can be extended to various fields like microelectronics, photoelectronic devices, chemical sensors and etc. For this reason, combining zeolite assembly techniques with microcontact printing, photoetching, and lithography techniques have an important scientific significance.

In the literature there are many patterning techniques for zeolite films attached on solid substrates are presented most of which are compatible with sensor technologies.

Huang et al. [53] used microcontact printing to produce zeolite patterns. Silicalite-1 suspension is dropped on a smooth surface. Then a patterned PDMS stamp is pressed on the suspension for 12h until the solvent is evaporated. Silicalite particles are attached to the smooth surface of the substrate with the capillary forces.

Yoon et al. [47] combined microcontact printing technique with self-assembly to covalently attach ZSM-5 crystals to the glass surface. This time PDMS molds were used to pattern the surface groups of the substrate. First of all PDMS stamps were placed on glass substrates to be able to pattern the octadecyl (OD) groups. Then the OD-patterned glass plates were dipped into a CP-TMS solution in toluene and refluxed for 3 h to link chloropropyl (CP) groups on the areas without OD groups. Afterwards, the glass plates were immersed into a ZSM-5 suspension and refluxed for 1 h. The areas on glass surface which has CP groups reacted with hydroxyl groups on zeolite crystals forming covalent linkage. The OD groups were not reacted with ZSM-5 crystals, and the areas with OD groups were remained uncovered.

Yoon et al. [46] also employed a similar technique which is a combination photolithography and self assembly. At first glass substrate is fully functionalized with IP-TMS and exposed to UV light through a mask. The uncovered IP groups were photochemically decomposed to hydroxyl groups, while the covered IP groups were still there. By immersing the glass plate in the synthesis solution, the continuous zeolite film would be grown on the hydroxyl group-covered part on the glass plate under hydrothermal condition.

CHAPTER 3

EXPERIMENTAL

3.1. Zeolite Immobilization and Patterning

3.1.1. Zeolite Immobilization

3.1.1.1. Spin Coating

For spin coating experiments, zeolite suspensions of 3 wt% in IPA was used. The zeolite suspensions were applied to the substrates and spun with 1500 rpm for 40 s. and dried in a furnace at 100 °C for 5 minute. These steps were repeated for three times on each substrate.

3.1.1.2. Ultrasonic Agitation

For ultrasound aided agitation experiments, zeolite suspensions of 3 wt% in toluene were prepared in glass tubes and agitated until they became homogeneously dispersed. Si substrates were dipped into the zeolite suspensions in toluene and ultra-sonicated using an ultrasonic bath for 10 min. Then the substrates were rinsed in acetone and dried using N₂ gas.

3.1.1.3. Direct Attachment

The methodology for direct attachment experiments was based on the literature report [52]. Si wafers were cut into 2 cm x 2 cm pieces and placed on a clean paper. About 2 mg of zeolite powder was put onto the substrates. Then they were pressed and rubbed onto the surface using a finger. Finally, the zeolite assembled Si wafer substrates were heat treated at 100 °C in a conventional oven for 30 min.

3.1.2. Zeolite Patterning

Various concentrations of PMMA were obtained by diluting PMMA C7 with chlorobenzene. 5 wt% and 7 wt% of PMMA were spun on Si wafers with 6000 rpm forming ~400 nm and ~850 nm thick resist films respectively. After coating the resist, substrates were pre-baked for 30 min at 160 °C. Patterns were defined by utilizing EBL system (Xenos XeDraw2 Pattern generator attached CamScan CS3000 SEM). Patterned substrates were developed in MIBK/IPA solution for 60 s, rinsed in IPA, washed in flowing pure water, and finally dried with N₂ gas. All zeolite attachment methods were applied to the PMMA coated Si wafers. The prepared thin films were put into an oven at 100 °C for 30 min. Then the substrates were rinsed and ultrasonicated in acetone and dried using N₂ gas. Degree of coverage was simply judged from SEM results. The binding strength was measured from the remaining zeolite particles on the Si wafers after ultrasonication for 30 s to 5 min in dry toluene [54-56]. Schematic representation of the procedure can be seen in Figure 3.1.

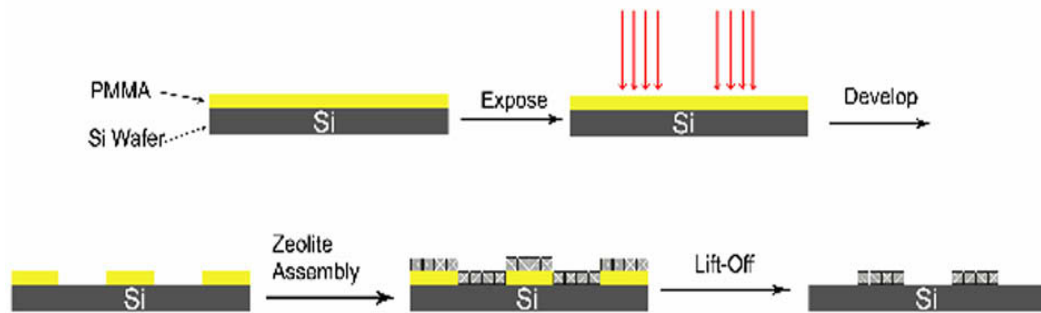


Figure 3.1: Schematic representation of the fabrication of zeolite nanocrystals on Si wafer.

3.1.3. Characterization

X-Ray diffraction (XRD) measurements were performed on a Rigaku Ultima 4 diffractometer using Cu K α radiation. The morphology of the synthesized zeolite nanoparticles and the zeolite thin films on Si wafers were investigated by FEI Quanta 400F field emission scanning electron microscope, operated at 30 kV. For FE-SEM observations, the samples were not coated. AFM measurements were conducted using Veeco Multimode V with Nanoscope V controller. Images were collected using tapping mode.

3.2. Biosensor Measurements

Materials: The frozen-dried preparations of enzymes used in the experiments were as follows: glucose oxidase (GOD) from *Penicillium vitale* (EC 1.1.3.4) with specific activity of 130 U/mg from *Diagnosticum* (L'viv, Ukraine); urease from soybeans (EC 3.5.1.5, type B) with activity of 22 U/mg from *Sigma-Aldrich Chemie*. Bovine serum albumin (BSA) (V fraction) and 50 % aqueous solution of glutaraldehyde (GA) were obtained from *Sigma-Aldrich Chemie*. Glucose and

urea were used as a substrate and analyzed substance, potassium-phosphate solution ($\text{KH}_2\text{PO}_4\text{-NaOH}$), pH 7.2 from *Merck* was used as a buffer. Other non-organic compounds were of analytical grade.

For electrochemical polymerization of enzyme the monomer 3,4-ethylenedioxythiophene (EDT) from “Baytron M” (Germany) and 50% polyethylene glycol from “Sigma” were used. Glutaraldehyde produced by “Fluka” was also used as a polymer matrix for enzyme deposition. Besides, the following chemicals are used for the experiments: glucose and bovine serum albumin (BSA) from “Sigma.”, hydrogen peroxide, ethanol, $\text{Na}_2\text{HPO}_4\cdot 7\text{H}_2\text{O}$ and KH_2PO_4 from “*Merck*”. All chemicals were of analytical reagent grade and used as received without additional purification.

Four different types of zeolites were tested during the whole study. These were zeolite Y, A, Beta and Silicalite. Some of them were commercial samples and some were synthesized in our laboratory. Different ion exchange procedures were conducted for zeolite Beta to have a preliminary idea about its effect on the conductometric and ISFET measurements. A short list of the zeolites used can be seen in Table 3.1.

Synthesis of zeolites and silicalite: Zeolite and silicalite particles were hydrothermally synthesized according to Table 3.1 and detailed synthetic conditions and reagents are listed. All the reagents were chemically or analytically pure and used without any purification. The particle size of zeolite crystals were determined using scanning electron microscope (SEM) are listed in Table 3.1. Morphologies of the particles can be seen in SEM images presented in Appendix A.

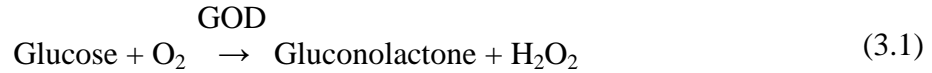
Table 3.1: List of zeolite samples and their synthesis procedures.

Zeolite Type	Chemical Composition of Gel	Pore Size* (nm)	Si/Al Ratio
Zeolite A	11.25SiO ₂ :1.8Al ₂ O ₃ :13.4(TMA) ₂ O:0.6Na ₂ O:700H ₂ O.	0.41	~ 1,35
Zeolite Y	Commercial	0.74	~ 2,39
Silicalite 2	1TPAOH:4TEOS:350 H ₂ O	0.53 x 0.56	No Al
Silicalite 1	1TPAOH:5TEOS:500H ₂ O	0.53 x 0.56	No Al
H ⁺ Beta 300	Commercial	0,76 x 0,64	~150
H ⁺ Beta 150	Commercial	0,76 x 0,64	~75
NH ₄ ⁺ Beta 25	Commercial	0,76 x 0,64	~12.5
Beta 30*	1,92 Na ₂ O : Al ₂ O ₃ : 30 SiO ₂ : 4,6 (TEA) ₂ O : 444 H ₂ O	0,76 x 0,64	~15
Beta 50*	1,92 Na ₂ O : Al ₂ O ₃ : 50 SiO ₂ : 4,6 (TEA) ₂ O : 444 H ₂ O	0,76 x 0,64	~25

* NH₄⁺, and H⁺ ion-exchanged Beta 30 and Beta 50 zeolites were also tested. Beta 30 and Beta 50 are in their Na⁺ forms.

Enzymatic Reactions

The key enzymatic reaction used for glucose determination by biosensor based on immobilized glucose oxidase is:



Substrate enzymatic transformation results in generating electrochemically active substance, hydrogen peroxide, decomposition of which causes formation of electrons measurable by means of amperometric transducer:



The key enzymatic reaction used for urea determination by conductometric and ISFET biosensors based on immobilized urease is:



3.2.1. Conductometric measurements

Sensor structure and measurement setup:

The conductometric transducers were produced in Lashkarev Institute of Semiconductor Physics of National Academy of Sciences of Ukraine (Kyiv, Ukraine). They were consisted of two identical pairs of gold interdigitated

electrodes made by gold vacuum evaporation onto pyroceramic substrate (5 x 40 mm). The surface of sensitive area of each electrode pair was about 1.0 x 1.5 mm. The width of each of interdigital spaces and digits was 20 μ m. Measurements were done by using a custom designed setup produced in METU Central Laboratory for this thesis work. A RTC872 model Lock-in Amplifier, a DACard embedded computer and appropriate connections are used and data are acquired and stored with the help of a program implemented in LabView program.

Bioselective membrane production:

%10 glycerol containing, 20 mM phosphate buffer with a pH 7.2 is used as the membrane solution. For the membranes on working electrode; 5% enzyme is added into membrane solution. For Reference electrodes same amount of BSA was added to membrane solution instead of enzyme to maintain the protein content of the membranes similar to working electrode.

Immobilization was carried out after deposition of 0.5 μ L of each solution on each electrode pair and then exposure to GA vapor. Before usage, the sensors were dried in air at ambient temperature for 10 min and then were exposed to the working buffer solution.

For zeolite added sensors, various amounts of zeolites were added into both reference and working membrane solutions. Solutions were sonicated until they became homogenous and applied to the electrode surfaces with the same method.

Zeolite coated conductometric electrodes

Instead of adding zeolites into bioselective membrane, electrode surfaces were directly modified by attaching zeolite particles onto the transducer surfaces. For this purpose bare conductometric electrode pairs were dipped into 10% silicalite solution and dried at 100°C in a conventional oven for 30 min.

Afterwards two different experimental procedures were investigated in comparison with the conventional methods. As the first experimental procedure working parts of the conductometric electrodes are exposed to 10% Urease in PBS solution for 80 min. Reference parts are not modified. Afterwards electrodes are washed with PBS and dried. As the second experimental procedure standard enzyme membrane solution and reference membrane solution were casted onto working and reference part of the zeolite coated electrodes respectively prior to the 25 min GA vapor exposure. Preliminary response curves were obtain from such electrodes for the first time.

The measurement procedure: The measurements were carried out in an open cell at room temperature. The 10 mM phosphate buffer or universal buffers at different pH values were intensively stirred. The necessary substrate concentration in the working buffer was achieved by adding given portions of the stock substrate solution. The experiments were repeated at least three times sequentially. The effect of nonspecific variations of output signal owing to temperature and pH changes and electric interferences was avoided by operating in the differential mode.

3.2.2. Amperometric measurements

Sensor structure and measurement setup:

All electrochemical experiments were performed using the traditional three-electrode system in which the printed electrode SensLab (SensLab GmbH, Leipzig, Germany) combines in itself all three electrodes - platinum working, auxiliary and reference [57]. Amperometric measurements at a constant potential were carried out in 5 mL electrochemical cell using potentiostate PalmSens (Palm Instruments BV, the Netherlands).

Bioselective membrane production:

Enzyme immobilization by electrochemical polymerization in the polymer poly(3,4-ethylenedioxythiophene)

Electropolymerisation of small monomers is a technique for the formation of a membrane at the electrode surface. It enables to select and maintain dimensions, shape and thickness of the matrix and to provide exact control over precipitation. Electropolymerised films can be successfully used in biosensors since these films, due to their permselectivity to hydrogen peroxide over other compounds, act as a selective barrier reducing interfering effect of electroactive substances. More detailed characteristic of poly(3,4-ethylenedioxythiophene) (PEDT) electrochemical polymerization can be found in the work published by Dzyadevych et. al. [57].

For electrochemical polymerization, the mixture of components consisting of 10 mM 3,4-ethylenedioxythiophene (EDT), 50% polyethylene glycol (PEG) and 30% enzyme solution, was prepared in 20 mM phosphate buffer, pH 6.2 for EDT and PEG solution and pH 7.2 for GOD solution.

PEDT was polymerized by application of the potential from +0.2 to +1.5 V at the rate of 0.1 V/s during 15 cycles using the potentiostat PalmSens. The PEDT electrochemical synthesis was monitored by cyclic voltammetry.

After the enzyme immobilization in PEDT the surface of SensLab electrode was washed with distilled water.

Enzyme immobilization in glutaraldehyde vapour

Glutaraldehyde is a polyfunctional agent which forms covalent bonds between biocatalytic particles or proteins. Therefore enzyme immobilization with glutaraldehyde is often used for development of enzyme biosensors. This immobilization method produces a three-dimensional matrix, in which the enzyme

is closely trapped with the electrode material, thus improving both retention of the biomolecule on the electrode surface and its electrical communication [58].

For formation of the glutaraldehyde-based bioselective membrane, a drop of 30% GOD solution with 5% BSA was put on the surface of working electrode. Then sensors were placed into glutaraldehyde vapour atmosphere during 10 min and dried in the air.

Experiments with zeolites

In the case of electrochemical polymerization zeolite solution was prepared in PEDT solution (only for Silicalite-1) or in PEG solution (for all other zeolites). Final zeolite concentration in membrane in all cases was 5%. Cyclic voltametry is applied to the electrodes.

In the case of enzyme immobilization in glutaraldehyde vapour zeolite solution was prepared in BSA solution. Final zeolite concentration in membrane was 5%.

The measurement procedure:

All measurements were performed in 20 mM K, Na-phosphate buffer solution, pH 7.2, at room temperature in an open bulk at intensive stirring. The glucose concentrations were changed in a controlled manner by adding certain aliquots of concentrated solutions. After each measurement, the biosensor was washed with buffer solution to stabilize the basic signal.

The storage stability of the developed biosensors was tested using dry storage of the sensor at +4 °C between the measurements.

3.2.2. ISFET measurements

Sensor Structure and measurement setup:

ISFET sensors are produced in Institute of Bioengineering of Catalunya utilizing microelectronic technology procedures. After production, sensors are packed in Lyon (CPE) and prepared for biosensor measurements. Measurements are conducted using a custom made electronic circuitry controlled by a computer and a software.

Bioselective membrane production and measurement procedure:

10% glycerol and 10% urease containing, 20 mM phosphate buffers with a pH 7.2 is used as the membrane solution. Immobilization was carried out after deposition of 0.5 μ L of membrane solution on ISFET electrodes and then exposed to GA vapor for 25 min. Before usage, the sensors were dried in air at ambient temperature for 10 min and then were exposed to the working buffer solution.

Two different measurements were made by ISFET electrodes. Basically, the responses gathered upon pH change and urea concentration change were recorded.

In order to make pH measurements ISFET electrodes are exposed two different solutions with different pH values. Responses to two different solutions were recorded.

For urea measurements, membrane coated ISFET sensors and the reference electrodes were dipped into cell filled with 40 ml 5 mM PBS. Various volumes of 150 mM Urea solution is added subsequently. After each addition, responses were recorded.

CHAPTER 4

RESULTS AND DISCUSSIONS

4.1. Zeolite Immobilization and Patterning

4.1.1. Zeolite Immobilization

The most efficient method for zeolite assembly on the Si wafers was tested using the three well established techniques, which are spin coating [59], ultrasound aided agitation [42], and direct attachment methods [52]. These methods had been previously tested using glass substrates, owing to the importance of forming zeolite films on such substrates for advanced applications. In none of these studies, nano sized zeolites were successfully attached onto the substrates efficiently. The efficiency criteria for the successful assembly of zeolite nanocrystals on the Si wafers were taken as full degree of coverage, strong binding, and organized assembly of zeolite particles with the ability to control zeolite patterns in the nanometer range. Organized assembly refers to having uniformly oriented and fully covered monolayers of zeolite nanocrystals.

4.1.1.1. Spin Coating

Spin coating materials onto substrates, in order to form thin films for practical applications, is the most well known and easy to use technique among the other ones. It should also allow effective control of the film thickness by varying the concentration of solution and the spinning rate. However, it is usually not easy to achieve full control over the exact location and thickness as well as the organization of nanocrystals on the substrates.

In order to test effectiveness of this technique to form zeolite thin films on Si wafers, different concentrations of zeolite A solutions in IPA were prepared. The results can be seen in Figure 4.1.

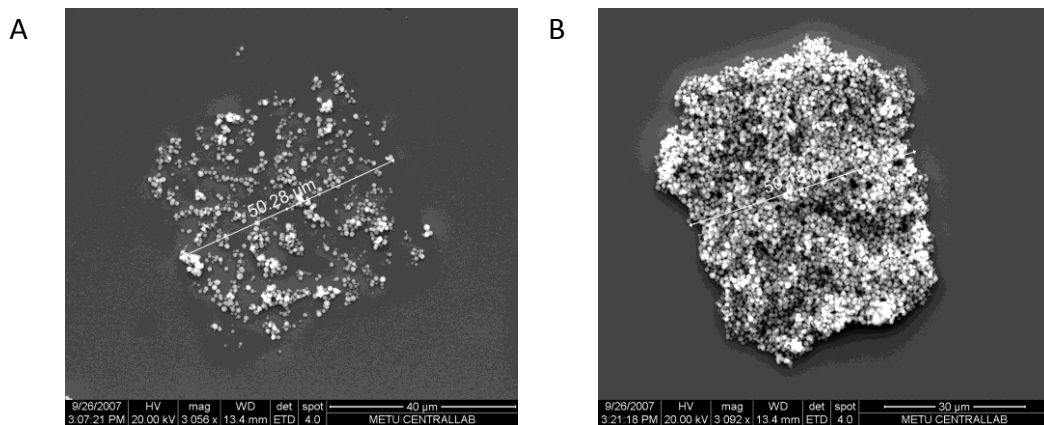


Figure 4.1: SEM images of spin coated samples. 1% zeolite concentration (A) and 10% zeolite concentration (B) in IPA.

As shown in Figure 4.1, at 1% zeolite concentration, substrate surface could not be fully covered. It was observed that zeolite concentrations of >5% (not shown) lead to full coverage, however all zeolite films were very thick and unorganized. Furthermore, most of the layers could easily be removed from the surface upon the substrate's contact with any solvent and slight sonication. Thus it can be concluded that spin coating the zeolites lead to more agglomerations and low surface coverage. The binding strength can be important for the use of the zeolite assembled substrates in real application areas, since these surfaces might be kept in different chemical/biological solutions and sonicated for immobilization purposes. In the current study, it can be inferred that the zeolite crystals are only weakly bound to the surfaces upon the application of spin coating method, since most of the crystals fell off rapidly from the substrates.

4.1.1.2. Ultrasonic Agitation

To be able to reduce the inefficiencies, encountered in spin coating method, ultrasonic aided agitation method was tested. In the literature, it is believed that ultrasonic agitation results higher degree of organization with the help of applied excess kinetic energy. For this purpose silanized Si wafers were dipped into zeolite solution prepared in toluene and ultrasonicated. SEM images can be seen in Figure 4.2.

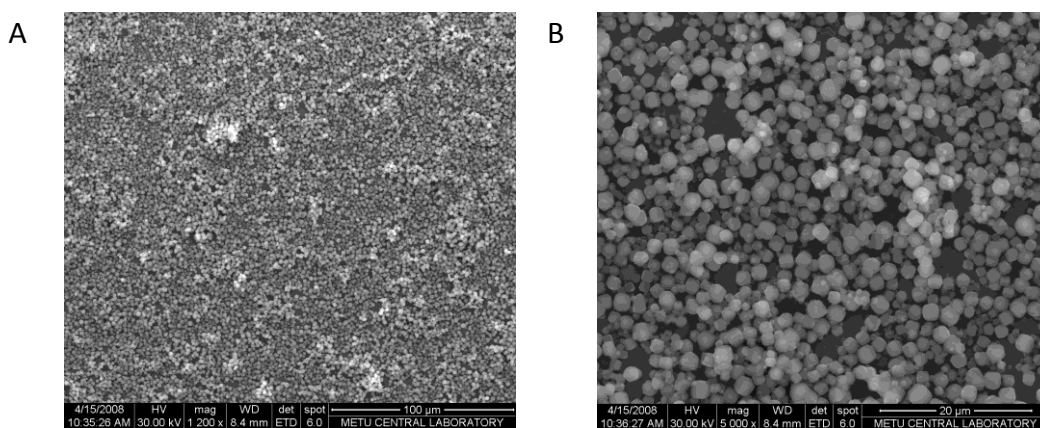


Figure 4.2: SEM low magnification (A) and High magnification (B) images of ultrasonic agitation samples.

As a conclusion, it was observed that ultrasound aided agitation method enhanced the formation of zeolite A monolayer. Furthermore, the agglomerated crystals on the very top layer before sonication fell off, and only the first layer bound onto the substrate was left after the sonication. Thus, although the number of crystals decreased down to 60% after 5 s sonication from the overall substrate surface, the percent coverage in the first monolayer was observed to decrease down to 30–45%. SEM images can be seen in Figure 4.2.

4.1.1.3. Direct Attachment

An alternative technique was developed by Yoon et al. to organize zeolites as monolayers on various substrates other than Si wafers [52]. It was hypothesized that “pressing” the microcrystals against the substrate and the forced migration of the crystals during rubbing are the two most important factors that led to the facile attachment of crystals on substrates with high degree of close packing. The

applicability of this method was shown in their study for microcrystals with the sizes between 0.5 and 12 μm and only on glass substrates.

In the current thesis study, direct attachment method developed by Yoon et al. for glass substrates and micron sized zeolite crystals was investigated to attach sub-micron zeolite A crystals on Si wafer substrates as an alternative approach for the first time [52]. The SEM image showing the results obtained after applying direct attachment method can be seen in Figure 4.3.

Figure 4.4 shows the SEM images comparing the efficiency of applying direct attachment method for attaching zeolites A nanocrystals on the Si wafers with respect to applying spin coating and ultrasound aided agitation methods.

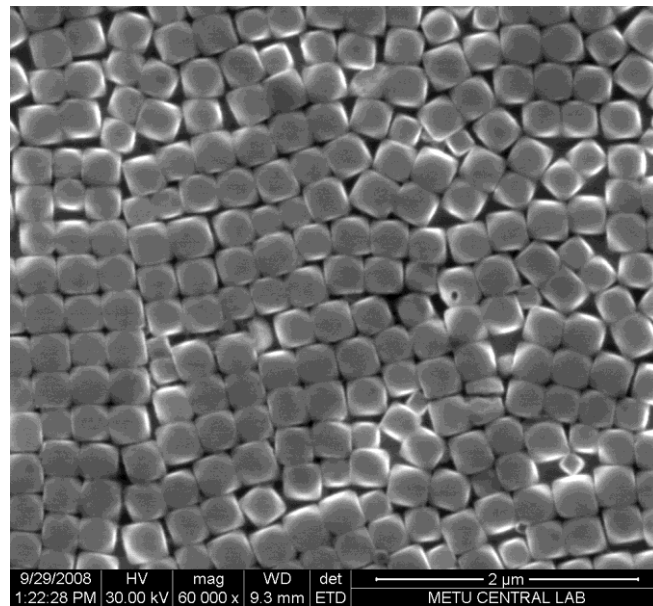
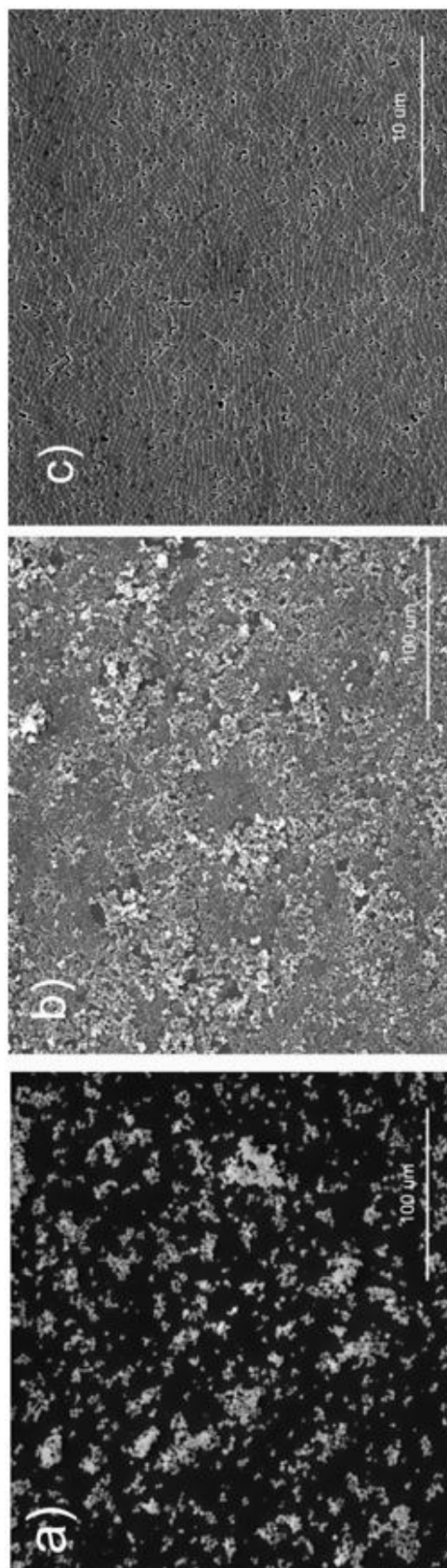


Figure 4.3: The SEM image showing the zeolites A attachment results obtained upon application of direct attachment method on Si wafer substrates.



F **Figure 4.4:** SEM images of zeolite immobilization experiments. a) Spin Coating b) Ultrasound aided agitation c) Direct attachment.

The desired criteria, which were stated as “full coverage” and “well organized monolayer” of zeolite nanocrystals on Si wafers were achieved upon using the direct attachment method. A general comparison of all techniques, i.e., spin coating, ultrasound agitation, and direct attachment is also shown in Figure 4.4.

Direct attachment method was previously found to be very suitable for the organized assembly of zeolite microcrystals with sizes between 500 nm and 12 μm by Yoon et al. on glass substrates [52]. In the current study, direct attachment method was shown to be successful in forming a monolayer of zeolite A nanocrystals with 200–250 nm size on the Si wafers and thus it was shown that this method can also be applicable for even smaller sizes of zeolites than 500 nm.

The preferred orientation of the zeolites A nanocrystals upon direct attachment method were investigated using XRD. As shown in Figure 4.5, after the application of the direct attachment method, zeolite A nanocrystals were shown to be oriented with a face of the cube parallel to the Si surface by the marked predominance of 100 crystallographic indexes.

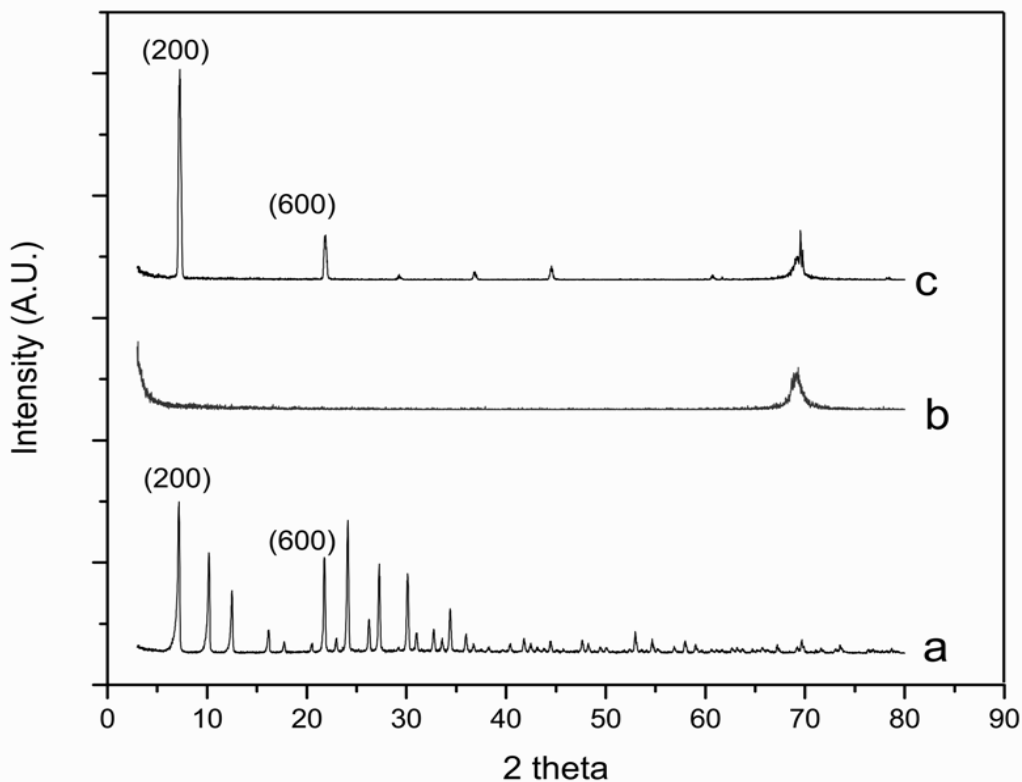


Figure 4.5: X-ray powder diffraction patterns of randomly oriented zeolite A nanocrystal powder (a), Si wafer (b), and uniformly oriented zeolite A nanocrystal monolayer on Si wafer after the application of direct attachment method (c).

In general, upon the application of direct attachment method, the number of zeolite A nanocrystals on the Si wafer substrates remained the same even after 5 min to extended periods of sonication. Thus, in the current study, “strong binding” refers to the fact that the remaining number of crystals was equal to the initially attached amount after sonication, leading to permanent attachment of zeolite A nanocrystals. Similar results were obtained by Yoon et al. using microcrystals as well [52]. Thus, application of direct attachment method on Si

wafer substrates was found to be an equally and sometimes more convenient technique with respect to the other traditionally used ones, such as layer by layer (LBL) assembly [60], ultra-sonication [42,52,55,61] and spin coating [59] methods, leading to high degree of coverage and uniform orientation of the nanocrystals.

Obtaining high degree of coverage depends on narrow and homogeneous size distribution of the crystals. Another factor that is important to be successful during direct attachment method is to be able to apply sufficient pressure by “pressing” onto the nanocrystals by allowing the crystals to migrate on the substrate. This observation is also in correlation with that of Yoon et al. [52]. Thus, it may not be as easy to apply the direct attachment method onto all types of polymeric surfaces as it is on smooth (slippery) surfaces [74]. In general, application of other techniques with chemical linkers can be relatively intricate for the purpose to developing such organized monolayers on very smooth, conductive surfaces like Si wafers. However, in this case the smoothness was an advantage for the application of the direct attachment of zeolite nanocrystals.

4.1.2. Zeolite Patterning

Compatible methodologies tested on Si wafer substrates, i.e., spin-coating, and direct attachment, were also tested for the purpose of producing patterns in the sub-micron scale with the combination of EB lithography. In the literature, facile methods for producing zeolite patterns on glass [62], ITO surfaces [63], and Si wafer [64] by microcontact printing and photolithography were studied previously.

These applications offer a potent methodology for their integration into devices such as bio-FETs, since zeolite micropatterns were suggested to be very durable, tailorable with controlled hydrophilic/hydrophobic properties, and CMOS compatible [64]. Microcontact printing was shown to form patterned stripes of zeolite monolayers with an average size of 3–55 μm [62, 63], and upon employing

photolithography, patterns with the smallest line widths of 5 μm were created [64]. Whether the degree of coverage and the orientation of zeolite microcrystal monolayers within such patterns can be improved or not was not investigated in those studies.

4.1.2.1 Pattern Formation by using Spin coating

The efficiency of using spin coating for forming zeolites A patterns on Si wafer substrates was investigated. Although, it was shown that spin coating was not a very beneficial technique to form zeolites monolayers on Si wafer substrates, its usability for inserting zeolites nanocrystals into the desired patterned locations was studied. An overall result representing the results obtained upon using spin coating can be seen in Figure 4.6.

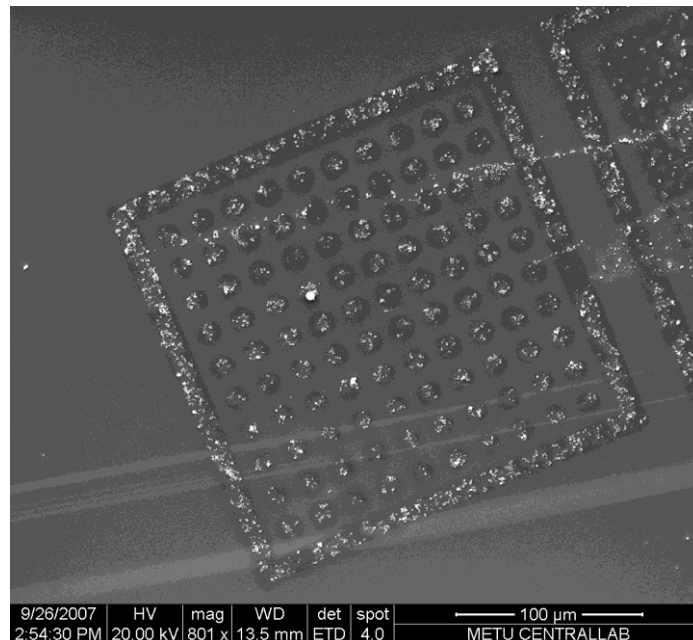


Figure 4.6: SEM image of the patterns generated by the combination of EBL and Spin Coating.

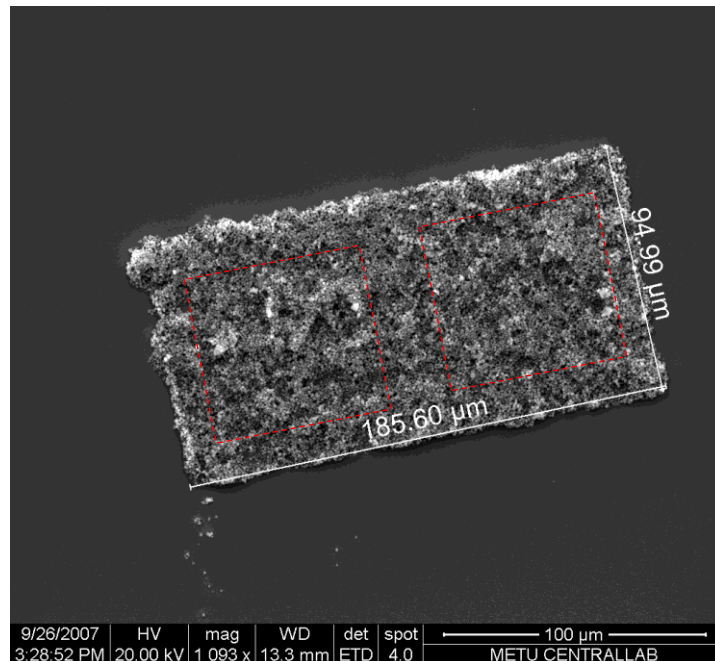


Figure 4.7: The SEM image showing the loss of all patterns formed on the Si wafer substrate upon the application of spin coating zeolites A crystals. The dashed lines show where the patterns were formed by EB lithography.

As shown in Figure 4.6, the zeolites could be inserted into the patterns formed by EB lithography. However, it was almost impossible to obtain a strongly bound, organized zeolites monolayers with controlled thickness using this method. In order to obtain full coverage in the patterns, increasing the concentration of zeolite A solution used for spin coating was also tested. As shown in Figure 4.7, increasing the zeolite A concentration to around 10% by weight lead to the disappearance of the zeolites patterns.

4.1.2.2 Pattern Formation by using Direct Attachment Method

Zeolite A nanocrystals were attached on the Si wafer according to the procedure described in the Section 4.1.1.3 and the zeolite micro-patterns that were formed on the Si wafer are shown in Figure 4.8.

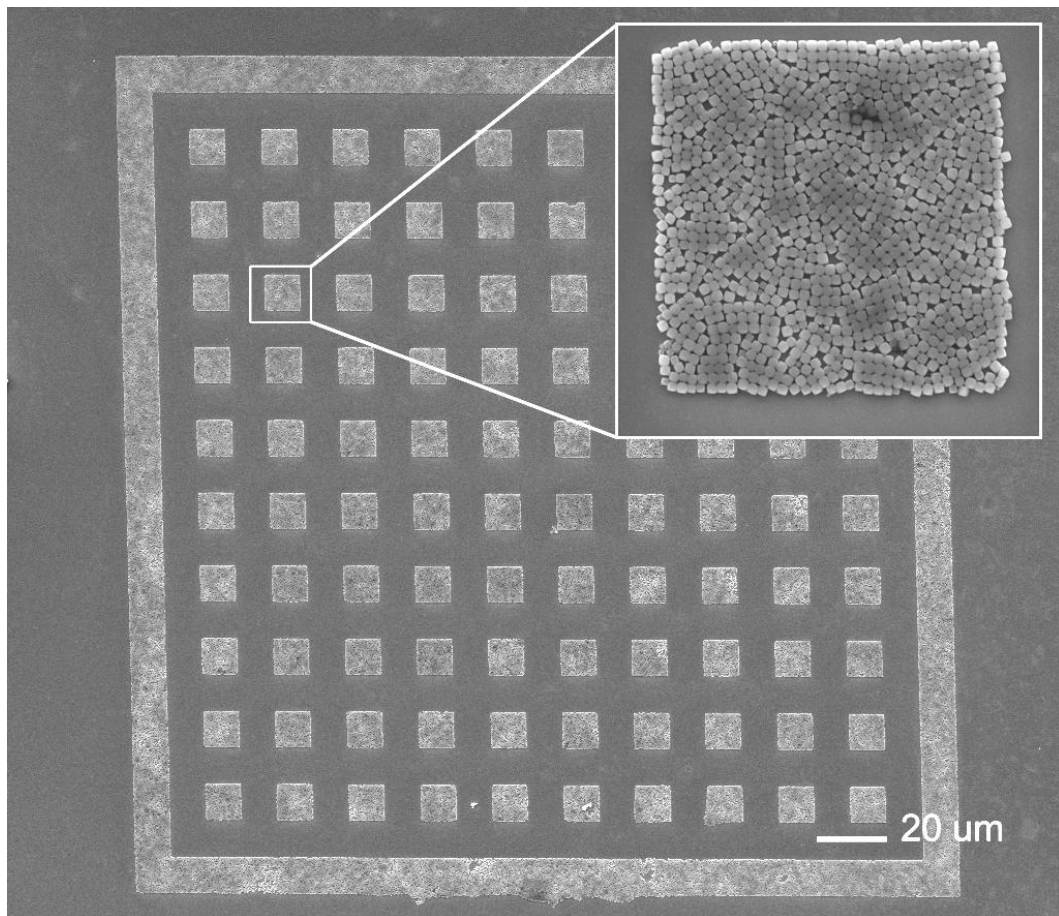


Figure 4.8: SEM image of zeolite micro-patterns on Si wafer obtained upon using direct attachment method.

According to these results, the combination of direct attachment method with EB lithography was observed to lead to an improved control over the organization of zeolites, shapes and features of the patterns in comparison with the other methods studied for similar purposes such as photolithography and microcontact transfer printing [62-64]. More specifically, Yoon [62] also obtained high coverage by functionalizing the substrate or zeolite surfaces; however the size of the patterns formed by photochemical pattern transfer method were around 2–70 μm . The monolayers formed by pattern transfer method were not as fully organized as the ones obtained in the current study by using direct attachment method [62]. By microcontact transfer printing, Cucinotta et al. obtained only 45% coverage for bare ITO substrates and up to 65% coverage for polymer coated substrates as determined from florescent microscopy [63]. No investigation on the binding strength was investigated. After 30 s sonication of the zeolite assembled Si wafer substrates upon spin coating, no matter whether the zeolites were bare or functionalized, almost no crystals were left on the substrates from what we observed using FESEM. Upon trying the ultrasound aided agitation method, the agglomerated crystals on the very top layer before sonication fell off, and only the first layer bound onto the substrate was left after the sonication. Sometimes, longer sonication times lead up to coverages <50%. When direct attachment method was used for the same purpose, the surface coverages obtained were always >90% in all trials on Si wafer substrates using zeolite A nanocrystals. Since direct attachment method does not necessitate the use of any chemicals, it was found to be a more suitable and practical technique for patterning purposes to be applied on Si wafers with respect to the mostly used ultrasound aided agitation method [61]. This is important, because application of direct attachment method does not harm the resist (PMMA) during processes requiring the use of lift off, whereas the traditional chemical linkers and their solvents used for similar purposes do harm the resist leading to the loss of patterns.

4.1.2.3 Formation of Line Patterns and Controlled Thicknesses of Zeolite A Nanocrystals using Direct Attachment Method

In the current thesis work, the limits of forming nano-micron sized stripes of zeolite A on Si wafers was tested to see if zeolite nanocrystals could be assembled on the Si wafers with high precision. Thus, several line widths were tested to see the minimum number of zeolites in a row that forms the line stripes. For that purpose, line widths in the range of 150nm – 10 μ m were patterned on Si wafer in a controlled manner using EB lithography technique. Following the same route described before, the obtained patterns of zeolite stripes on the Si wafers are shown in Figure 4.9. According to the SEM images of the line stripes obtained in several different thicknesses (Figure 4.9b and 4.9c), the features of the patterned stripes can be as small as the zeolite size (Figure 4.9b) upon the combination of direct attachment method with EB lithography. To the best of our knowledge, the current study shows that the limit of the pattern resolution can be defined by the size of the zeolite nanocrystal for the first time. However, this result can only be drawn for zeolites with identical edge lengths such as zeolite A.

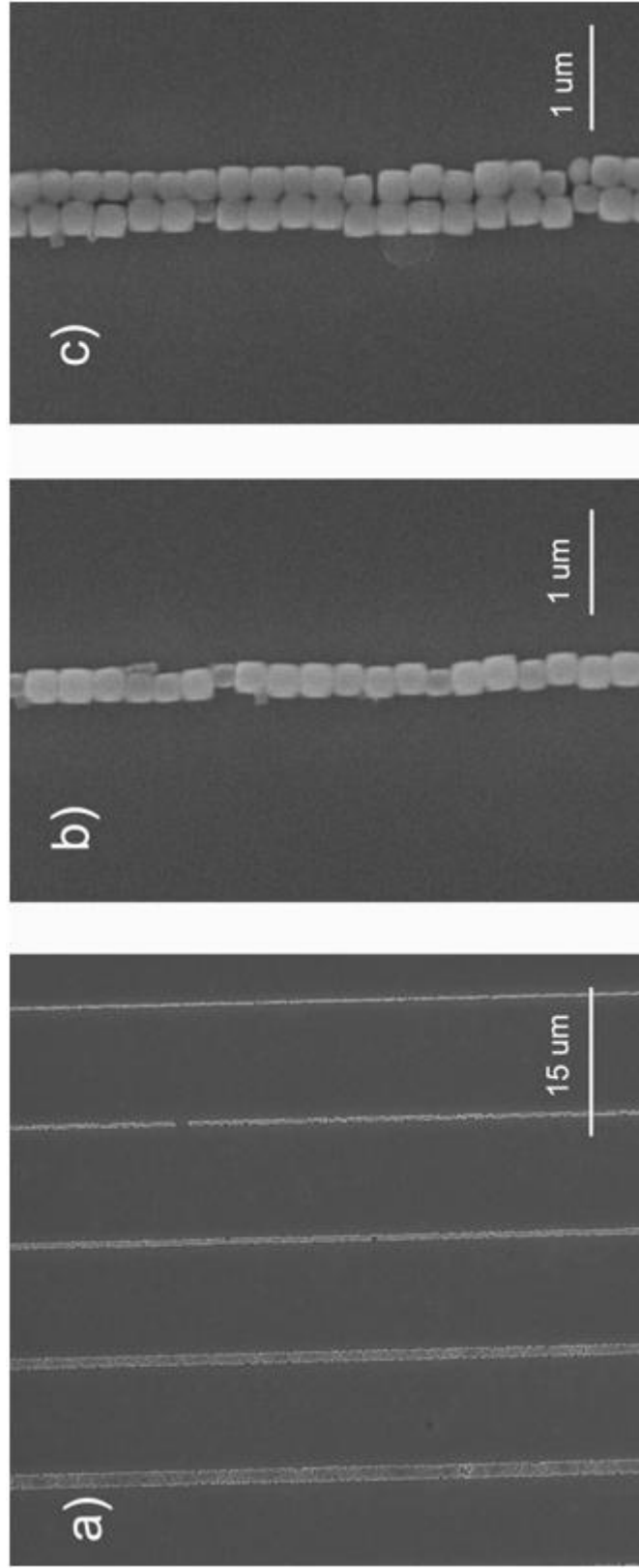


Figure 4.9: SEM images of monolayers of zeolite A nanocrystal stripe patterns with different line widths on Si wafer (a), and high magnification images of zeolite stripes formed of single (b) and double zeolite rows (c).

Furthermore, we investigated the possibilities of forming double layers of zeolite nanocrystals on the Si wafers using the direct attachment method. Traditionally, in situ synthesis and LBL assembly of zeolites are the two techniques that are used to prepare zeolite films on different substrates. However it can be hard to precisely control the zeolite thickness via in-situ synthesis, and the operation in LBL assembly is usually time consuming [65]. In the current study, since no chemical linkers were used throughout the process, we were able to form any patterns of interest not only by controlling the number of zeolite nanocrystals in a row, but also the number of zeolite layers. As shown in Figure 4.10, it was found that the thickness of the resist (PMMA) during the EB lithography was the dominating factor in order to successively control the number of zeolite nanocrystal layers on the Si wafers. Thus, we were able to show for the first time that the developed technique allows the control over forming a mono or double layers of zeolite A nanocrystals on the substrates for patterning purposes as well.

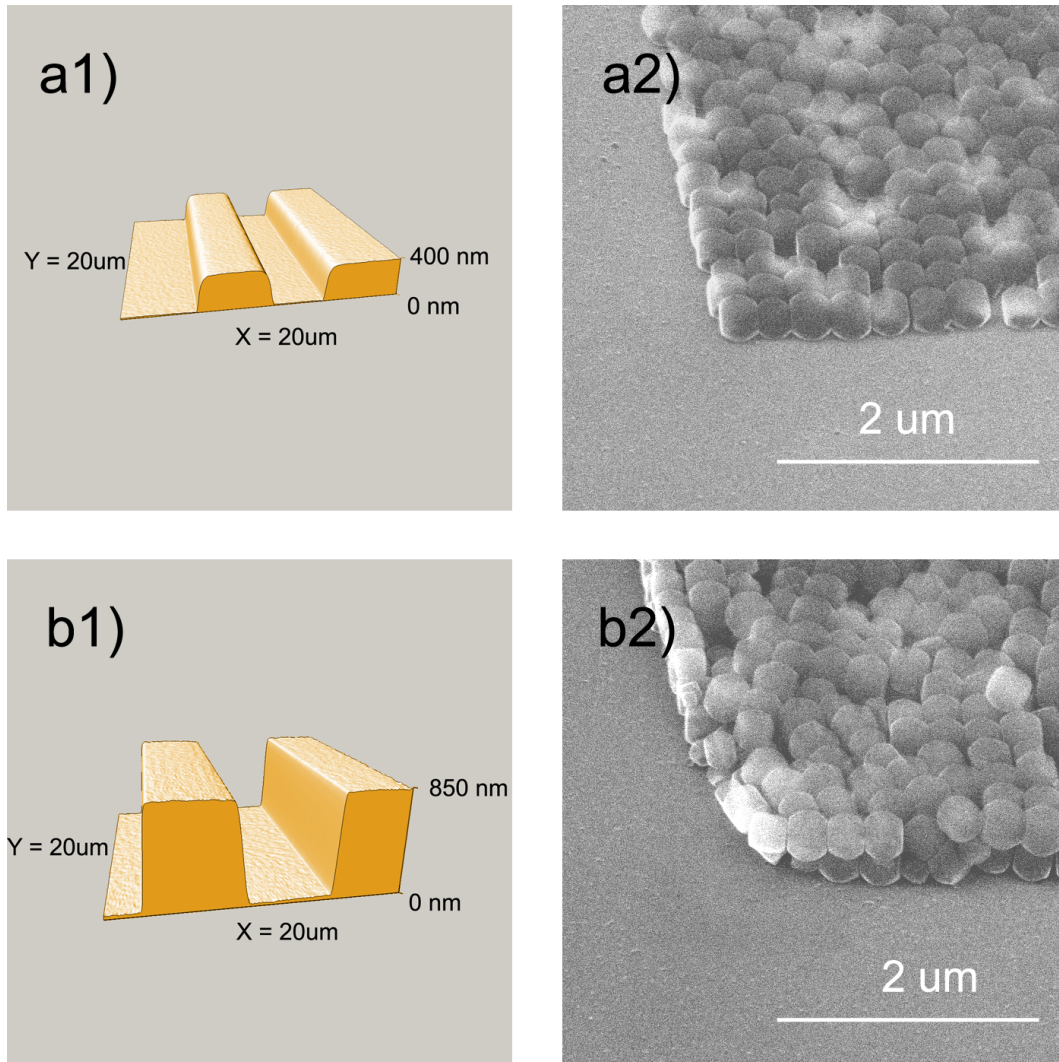


Figure 4.10: AFM images of ca. 400 and 850 nm PMMA coated and developed Si wafers (a and c); SEM image of zeolite monolayer on the developed Si wafer with 400 nm (b) and SEM image of zeolite double layer on the developed Si wafer with 850 nm (d) PMMA resist.

Since direct attachment method is basically rubbing zeolite nanocrystals on the Si wafer which is coated with the resist, there is a strong possibility to remove the resist during the zeolite attachment as well. Thus, it was beneficial to keep the resist thickness higher than the total height of the attached zeolite mono/double layer in order to achieve very organized sheet of zeolite nanocrystals. Accordingly, PMMA resists of ca. 400 and 850 nm thicknesses were coated on the Si wafers after which the process shown in Figure 3.1 was applied in the usual manner. Changing the thickness of the resist allowed us to make organized and closely packed single and double layers of zeolite nanocrystals as shown in Figure 4.10. It was observed that a monolayer of zeolite A nanocrystals were formed on a 400 nm resist coated Si wafer. When 850 nm resist was coated, the zeolites assembled on the developed patterns formed a double layer. These nanocrystals were also very strongly bound to the surface. As a result, it was shown for the first time that controlling the thickness of the PMMA resist can be used as an alternative and easy way to control the number of nanocrystal layers with no need for the incorporation of chemical linkers.

4.2. Biosensor Measurement Results

In this part of the study three different types of biosensor transducers were tested with conventional and zeolite added membranes. In general response magnitudes, linear dynamic ranges, storage and operational stabilities are important biosensor properties. In the current study most of these biosensor performances were investigated for conductometric, amperometric and ISFET type biosensors. In the literature, similar studies were made using commercial zeolite samples. However, this limits the ability to tailor the properties of zeolite surface groups. Thus in the current study, both commercial and laboratory synthesized zeolite samples were tested. Zeolite Beta was specifically chosen for ion exchange studies because it is the only type that can exist with such a broad range of Si/Al ratio. These zeolite samples were only tested with conductometric and ISFET type biosensors. The zeolite modified electrodes were only tested for conductometric measurements.

4.2.1. Conductometric measurement results

4.2.1.1 Effect of zeolite loading into bioselective membranes

Initially the effect of the zeolite loading in immobilization mixture on biosensor response to 8 mM urea was investigated. 5 wt% zeolite loaded enzyme membranes were tested with different zeolite types to understand the effect of zeolite on biosensor responses. Schematic representation of standard membranes and zeolite added membranes can be seen in Figure 4.11. Responses of the electrodes prepared with this procedure are summarized in Figure 4.12.

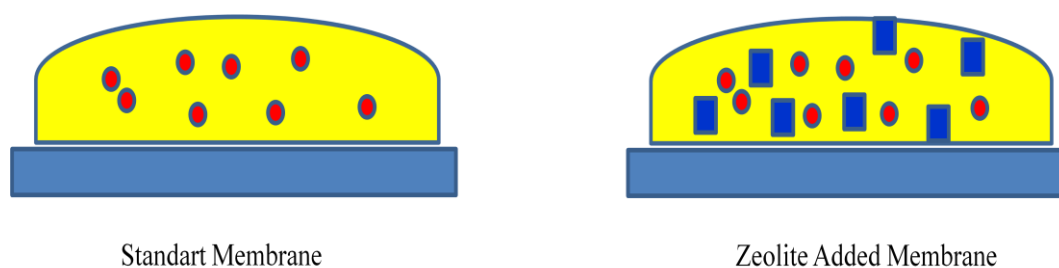


Figure 4.11: Schematic Representation of standard membranes and zeolite added membranes.

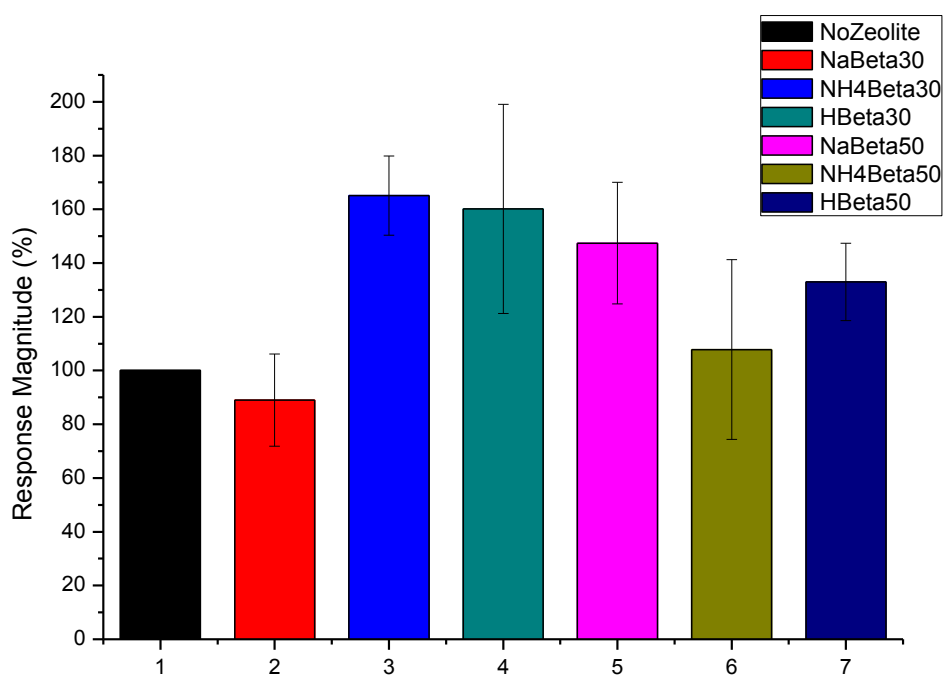


Figure 4.12: Normalized responses of conductometric urease biosensors to 8 mM urea without and with different types of zeolites. Na^+ -Beta-30 (1), NH_4^+ -Beta 30 (2), H^+ -Beta 30 (3) , Na^+ -Beta 50(4), NH_4^+ -Beta 50(5), H^+ -Beta 50 (6)

As shown in Figure 4.12, almost all zeolite added membranes lead to an increased response with respect to the ones obtained from no zeolite containing membranes. It seems that application of certain ion-exchange protocols to the as-synthesized zeolites (Na^+ -Beta) results in a relative increase in the responses. The purpose of this preliminary study was to see whether some control over the responses could be obtained by using ion-exchanged zeolites. Although, the reasons underlying behind the obtained variety of responses could not be explained at the moment, it can generally be concluded that an increase in the Si/Al ratio leads to an increased response in conductometric measurements (Figure 4.12, data points 1 versus 6), and it might be possible to controllably change the responses obtained from different biosensors by using diversely treated zeolite samples.

4.2.1.2 Results of zeolite film coated electrodes

Zeolite coated conductometric electrodes were investigated with urease enzyme for urea determination. Results of the experiments were compared with the standard membrane technique. Schematic representation of electrodes and calibration curves can be seen in Figure 4.13 and 4.14

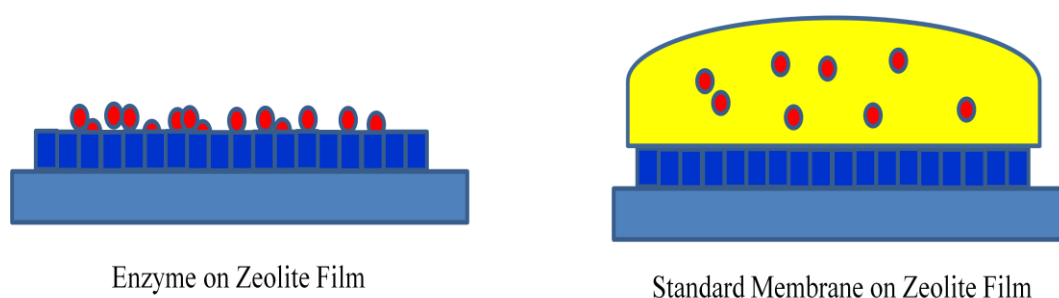


Figure 4.13: Schematic representation of zeolite film coated electrodes.

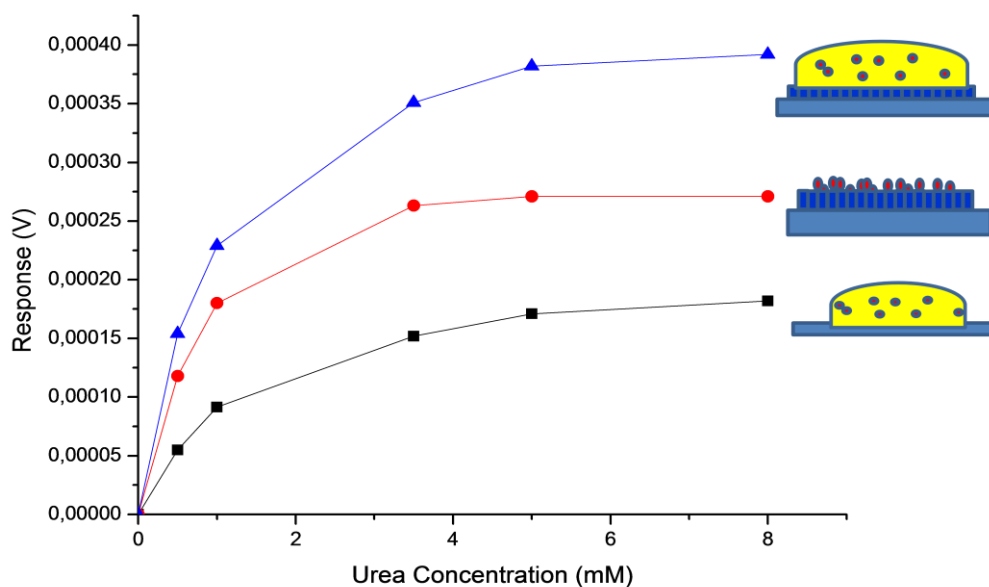


Figure 4.14: Calibration curves for urea determination for conductometric biosensors based on urease using enzyme membrane on zeolite film (1), enzyme on zeolite film (2) and standard enzyme membrane (3)

As shown in Figure 4.14, attaching zeolites on the electrodes and thus modifying the electrode surfaces with zeolite nanocrystals lead to an increased response in both cases of “enzyme on zeolite films” (Figure 4.14-2) and “enzyme membrane on zeolite films” (Figure 4.14-1). Although, this had been a first time investigation of such an approach for modified electrodes in urease measurements using conductometric biosensors, the investigations of the underlying reasons should be investigated in more detail in future studies.

A typical dependence of the conductometric biosensor response on the time after urea addition is also shown in Figure 4.15. As it can be seen in Figure 4.15 after the biosensor reached a stable value in blank phosphate buffer solution, injection of urea stock solutions caused significant sensor response, which resulted from subsequent local increasing of concentration of ionic species around transducer surface. As it can be seen the biosensor steady-state response times, i.e., times necessary to reach 90 % of the steady-state amplitudes, responses obtained from the zeolite modified electrodes significantly reduced from 1-2 min to about 5-10 sec.

For the standard membranes on zeolite films (Figure 4.15-1) responded in a similar way with the standard membranes (Figure 4.15-3). On the other hand, physically adsorbed enzymes on zeolite films (Figure 4.15-2), responded to substrates (urea) significantly faster than the other techniques. It can be hypothesized that the reason for the observed significant decrease in the time spent to reach equilibrium response values after the injection of urea is due to the reduced diffusion barriers. Polymeric membranes (Figures 4.15-1 and 4.15-3) can be thought of polymeric films behaving like diffusion barriers for substrates and products, which results in a delay to reach the equilibrium. For the case of physically adsorbed enzymes as shown in Figure 4.15-2, there are no limiting factors for the diffusion. This property can be important for applications, which require fast responding sensors.

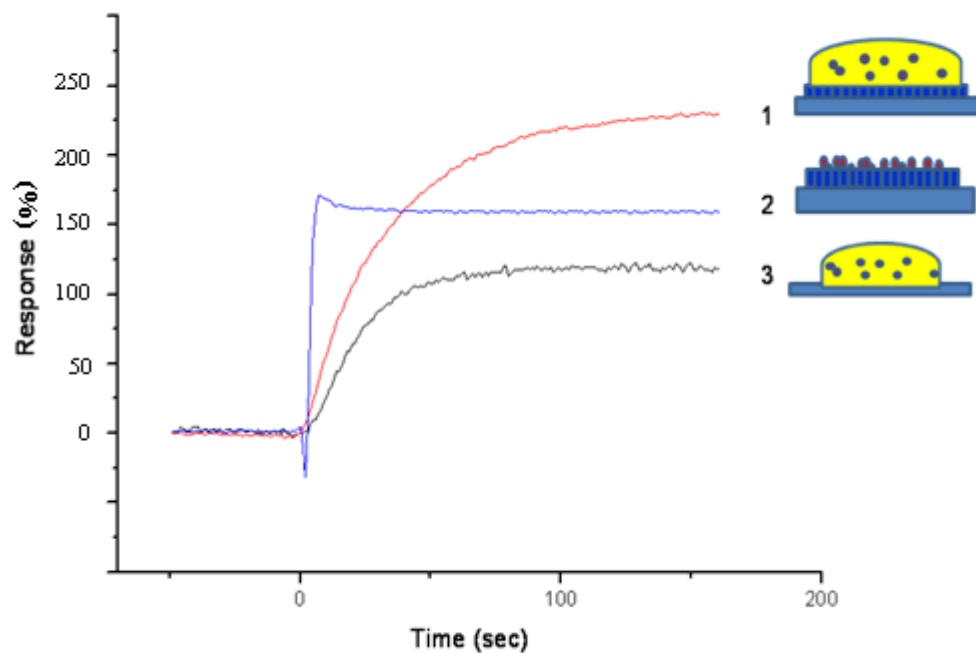


Figure 4.15: Typical response curves of conductometric biosensor based on urease using enzyme membrane on zeolite film (1), enzyme on zeolite film (2) and standard enzyme membrane (3) for 0.5 mM urea

4.2.2. Amperometric measurements results

Two different methodologies for immobilization of glucose oxidase (GOD) with silicalite samples of two different sizes were investigated. These are electrochemical polymerization in the polymer poly(3,4-ethylenedioxythiophene) (PEDT) and immobilization in BSA-containing membrane in glutaraldehyde (GA) vapor. The difference between silicalite-1 and silicalite-2 are their morphologies. The results obtained using immobilization of GOD in GA and PEDT with silicalite can be seen in Figure 4.16.

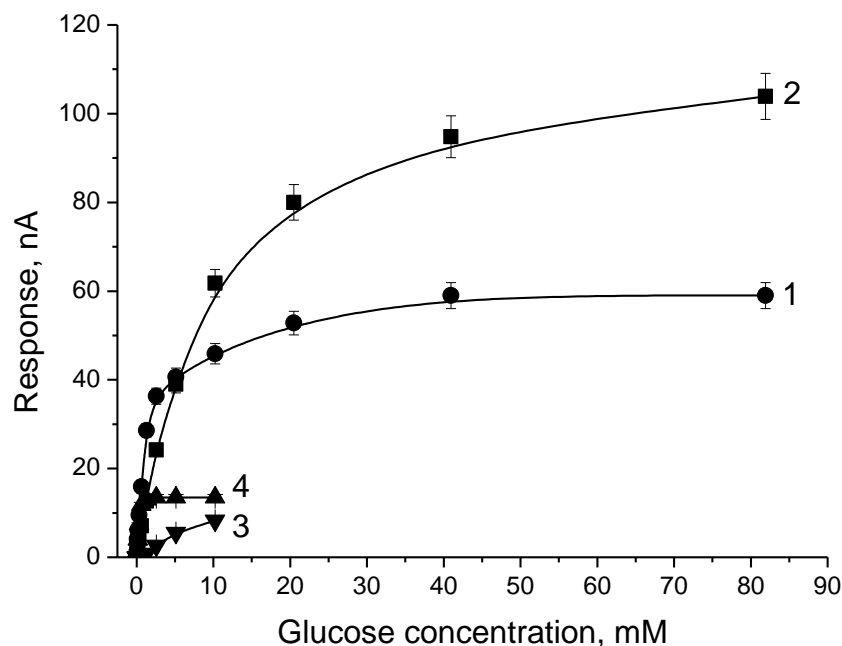


Figure 4.16: Calibration curves of amperometric biosensors based on platinum printed SensLab electrode with GOD with Silicalite-1 immobilized in PEDT (1) and in GA (3) and GOD with Silicalite-2 immobilized in PEDT (2) and in GA (4). Measuring conditions: 20 mM phosphate buffer, pH 7.2, at potential of +200 mV versus intrinsic reference electrode.

According to Figure 4.16, GOD electrochemical polymerization with zeolites in PEDT leads to biosensors with wider dynamic range of work and higher level of the signal. Thus, PEDT polymerization was chosen for the preparation of zeolite membranes on the electrodes and immobilization of enzymes for the rest of the studies. Also, it was observed that different morphologies of zeolite crystals lead to different responses. Accordingly, laboratory prototypes of glucose amperometric biosensors based on platinum printed electrodes SensLab and GOD immobilized in the PEDT with different zeolites and without zeolites were created. In all cases including zeolites, it was observed that GOD was active after immobilization with 5% zeolite solution

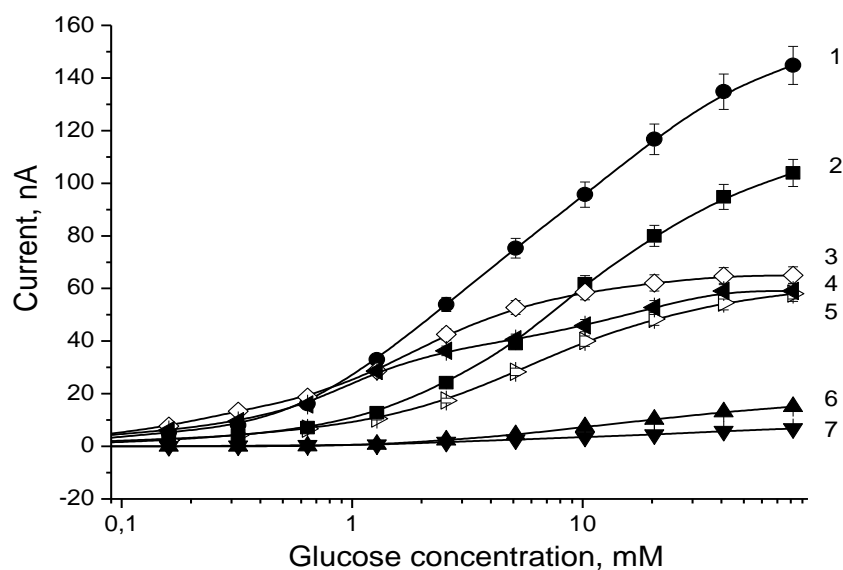


Figure 4.17: Calibration curves of glucose amperometric biosensors based on GOD without zeolite (4) and GOD with zeolites Silicalite-1 (1), Silicalite-2 (2), NH_4 -Beta-25 (3), Na-Beta (5), H-Beta-300 (6), H-Beta-150 (7), immobilized in PEDT. Measuring conditions: 20 mM phosphate buffer, pH 7.2, at a potential of +200 mV versus intrinsic reference electrode.

The calibration curves of the laboratory prototypes of amperometric biosensors based on GOD without zeolite and GOD with various zeolites are shown in Figure 4.17. Analysis of working characteristics of developed biosensors demonstrated linear response to glucose using GOD immobilized in PEDT with zeolites H-Beta-150 and H-Beta-300 in almost the same concentration range as GOD immobilized in PEDT without zeolite. The detection limit for these biosensors was 0.32 – 0.64 mM of glucose. However, in the case of GOD immobilization with other investigated zeolites, biosensors with smaller detection limits within the range of 0.01 to 0.04 mM of glucose were obtained.

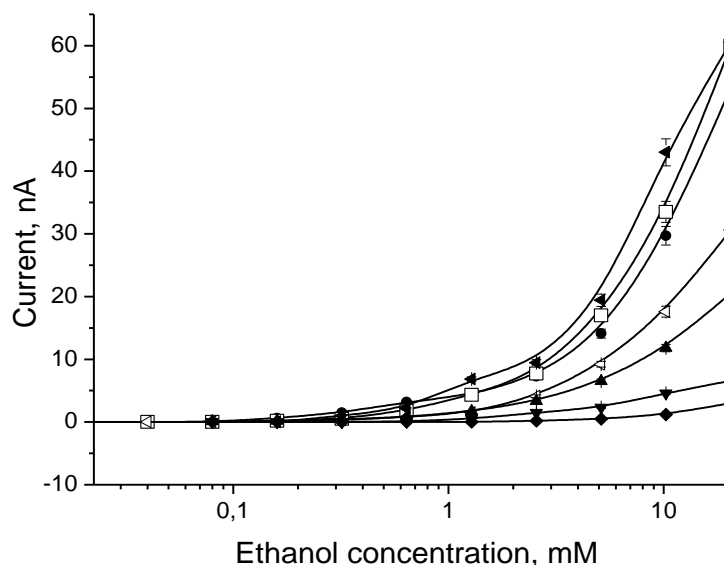


Figure 4.18: Responses of glucose amperometric biosensors to ethanol based on GOD without zeolite (4) and GOD with zeolites Silicalite-1(1), Silicalite-2 (2), NH₄-Beta-25 (3), Na-Beta (5), H-Beta-300 (6), H-Beta-150 (7), immobilized in PEDT. Measuring conditions: 20 mM phosphate buffer, pH 7.2, at a potential of +200 mV versus intrinsic reference electrode.

It is well-known that investigation of the selectivity of biosensors is important prior to application of these devices in analysis of real samples. Thus responses of developed glucose biosensors to ethanol, which is one of the main interfering substances, were also studied. The signals to ethanol of biosensors obtained upon using different zeolites are shown in Figure 4.18. As can be seen, unselective responses to ethanol of biosensors based on GOD without zeolite and GOD immobilized with both of the silicalite samples are almost the same. Sensors based on zeolites H-Beta-300, 150 and Na-Beta demonstrate lower responses to ethanol but their signals to glucose are also not high (see Figure 4.17). The best proportion of glucose and ethanol signals was observed for GOD immobilized with NH₄-Beta-25 and the selectivity of this biosensor was the best in comparison

with other devices. It can be hypothesized that Al content is important to achieve high selectivity in the current biosensor, since almost no change of selectivity was observed upon using silicalite samples. Usually silicalite is the typical material that is used in most immobilization studies, due to their high hydrophobicity and larger pore dimensions [66]. However, selectivity is also an important parameter to consider in biosensors especially for real samples analysis [58]. Thus, it does not seem that silicalites are the promising candidates if one aims to achieve the optimum selectivity as well. Furthermore, the current study showed that ion exchange procedures (H^+ , ammonia exchange) applied to the zeolite samples can be of importance to achieve the desired selectivity.

Table 4.1: Summary of zeolite modified amperometric biosensor results.

Zeolite	Immobilization method	Dynamic range, mM glucose	Response at saturation, nA	Response at ethanol, % of 20 mM glucose response	Storage stability	Operational stability
Without zeolite	GA vapor	0.08 – 1.28	37	8,6	100% after 2 months	118% after 8 hours
	PEDT	0.64 – 20	34	39	62% after 10 days, 35% after 20 days	
Silicalite-2	GA vapor	0.16 – 10	7	73	22% after 9 days	100% after 4 hours
	PEDT	0.02 – 5	75	29	83% after 16 days	70% after 8 hours
Silicalite-1 (spherical)	GA vapor	0.04 – 1.28	20	290	2% after 5 days	25% after 5 hours
	PEDT	0.04 - 10	62	100	14% after 8 days	57% after 8 hours
H ⁺ Beta 300	PEDT	0.64 - 10	7	200	77% after 7 days	
H ⁺ Beta 150	PEDT	0.32 - 10	3.5	146	23% after 4 days	
NH ₄ ⁺ Beta 25	PEDT	0.02 – 5	53	5	64% after 5 days	
Beta 12	PEDT	0.01 – 10	40	63	50% after 2 days	

The storage stability of all developed biosensors was also investigated and results are shown in Table 4.1. Activity of biosensors based on GOD immobilized with zeolites Silicalite-2 and H-Beta-150 rapidly decreased during first 4 – 5 days after immobilization. GOD immobilized in the PEDT without zeolite was not highly stable as well. It was observed that 70% of initial response was maintained in the first week and 38% in the second week of storage. GOD immobilized with NH₄-Beta 25 demonstrated similar stability: 64% of initial response in 5 days of storage. However, upon using H-Beta-300 and Silicalite-1, storage stability of the created biosensors was much higher. The developed devices demonstrated around 100% and 75% of the initial signal respectively during the first week after immobilization. With these zeolite samples, higher reproducibility was obtained as well with respect to the rest of the zeolite samples. From these results, it can be concluded that low Al content is important to achieve high stability. Also, the particle size of Silicalite-1 crystals are about twice as much of the Silicalite-2 crystals (Appendix I). Thus, particle size seems to be important when the same type of crystal with two different particle sizes is compared.

Results of comparative analysis of glucose amperometric biosensors based on GOD immobilized in the PEDT without zeolite and with different zeolites are shown in Table 4.1. As can be seen, biosensor with GOD and Silicalite-1 demonstrates the best working characteristics: low detection limit, high level of response, high storage and operational stability and sufficient selectivity. Biosensors with NH₄-Beta-25 and Na-Beta also have their advantages: low detection limit for both biosensors and very high selectivity to the substrate for NH₄-Beta-25 based biosensor.

These results suggest that zeolites of different types can be used as alternatives for GOD immobilization in amperometric biosensors development. It was shown that different zeolites with different characteristics lead to different biosensor results. Thus, it can be hypothesized that different properties of zeolites, such as their ion exchange behaviors, particle sizes, surface groups, pore sizes, and Si/Al ratios can be tailored in such a way that the optimum performance from a biosensor can be

achieved upon choosing the right zeolite type and tuning its characteristic properties. Accordingly, our future research will focus on to evaluate such zeolite characteristics in detail for potential development of the optimum electrodes for desired purposes.

4.2.3. ISFET measurement results

4.2.3.1. Effect of zeolite loading on pH sensitivity

ISFET transducers are pH sensitive devices even if they are not functionalized with bioselective elements. They give different responses to environments which has different pH values. To be able to understand the effect of zeolite loading on pH sensitivity a series of experiments were conducted. Six different types of zeolite added membrane solutions were casted on ISFET transducers without enzymes. Responses of transducers to pH changes were measured and compared with blank and BSA loaded transducers. Results of this experiment can be seen in Figure 4.19.

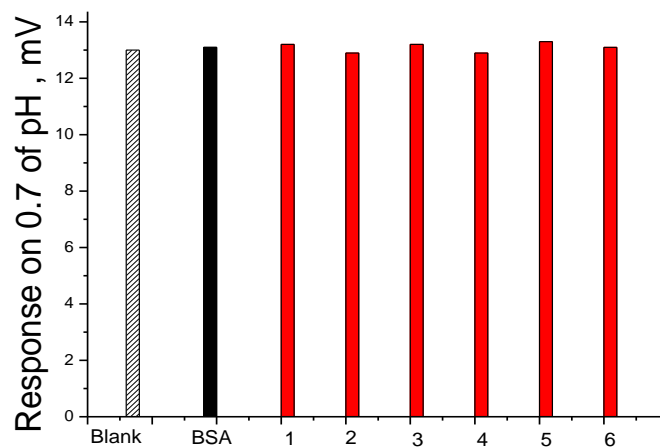


Figure 4.19: Response to pH change for different zeolites. -Beta-30 (1), NH₄ -Beta 30 (2), H⁺-Beta 30 (3) , Na⁺-Beta 50(4), NH₄ -Beta 50(5), H⁺-Beta 50 (6)

According to the results seen in Figure 4.19 no considerable changes can be seen in pH sensitivity. This is important to conclude that any changes in the biosensor performances are not related with the increase or decrease in the pH sensitivity of transducers.

4.2.3.2. Zeolite added Enzyme Membrane Results:

After the pH sensitivity experiments, “the effect of zeolite in enzyme membranes” was investigated. Six different types of zeolites were used during the experiments. The membrane solutions were prepared as mentioned in the previous section. Results were compared with the results of membranes without zeolites. All the experiments were done using the same electrode and repeated 4-5 times. Relative response magnitudes can be seen in Figure 4.20.

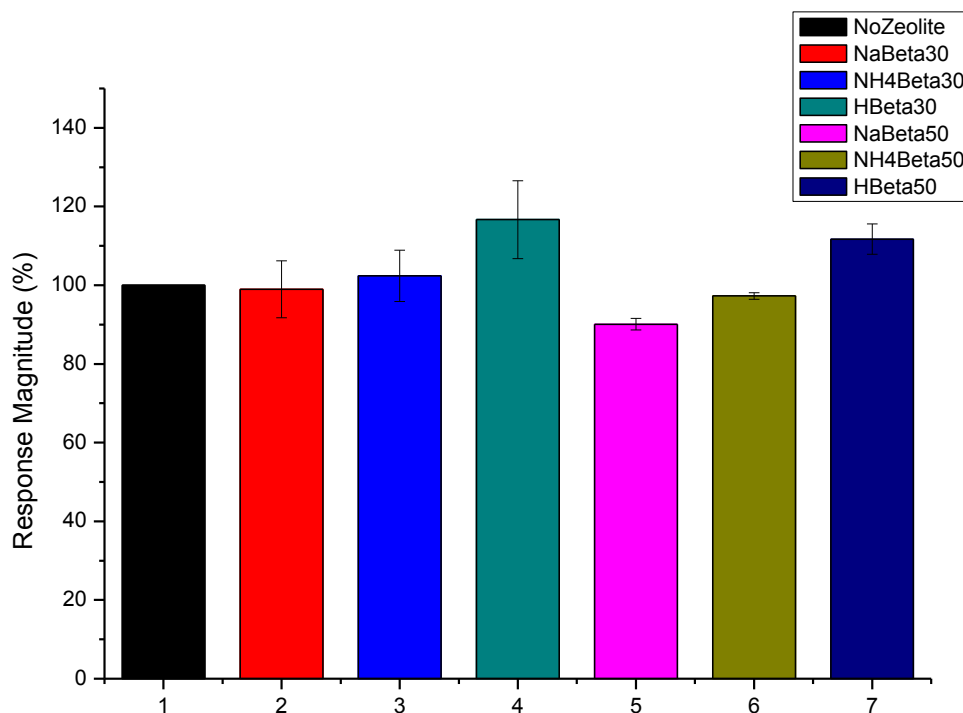


Figure 4.20: ISFET responses to urea using different zeolites. Na-Beta-30 (1), NH₄⁺-Beta 30 (2), H⁺-Beta 30 (3), Na⁺-Beta 50(4), NH₄⁺-Beta 50 (5), H⁺-Beta 50 (6)

In Figure 4.20 it is seen that different zeolite types modified the sensor signals in different ways. It was observed that zeolite 3 and zeolite 6, which are H⁺ exchanged zeolites in both cases, increased the signal significantly. On the other hand, zeolites 1 and 4, which are the as-synthesized zeolites in their Na forms, were observed to lead to reduced signals. These results showed that H⁺-Beta type zeolites have a positive contribution on signal where NH₄⁺-Beta type Na⁺-Beta type zeolites have a negative contribution. From this graph one can also conclude that Si/Al ratio (Beta-30 (Si/Al=30) versus Beta-50 (Si/Al=50)) also leads to a change in the response signals.

Furthermore, repeatability of measurements was also investigated. For this purpose, standard membrane solution and zeolite H⁺Beta-50 added membrane solutions were casted on transducer surfaces. After each immobilization, sensor surfaces

were cleaned and each experiment was repeated 10 times using the same electrode. Results of different immobilizations can be seen in Figure 4.21.

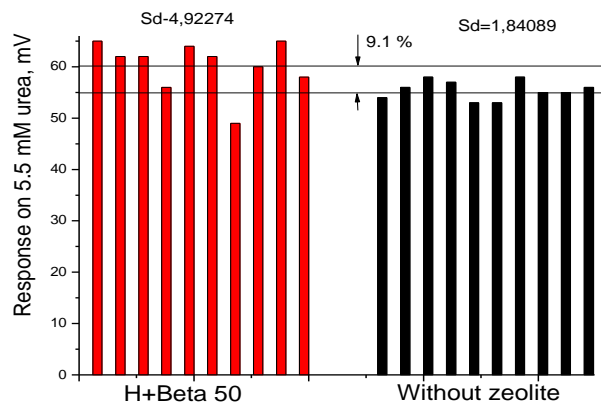


Figure 4.21: Repeatability experiment results for standard and zeolite added membranes.

Standard deviations of standard membrane and zeolite added membranes are found to be 1.8 mV and 4.9 mV. These standard deviation values are reasonable for ISFET type electrochemical sensors. On the other hand 9.1% higher response in average was achieved with the zeolite added membranes.

In general, all biosensor results suggest that zeolite addition into the enzymatic membranes lead to different results, which do change with different types, Si/Al ratio, and ion-exchange properties of zeolites. In most cases, it can be hypothesized that certain types of zeolites showed improved ISFET performances. On the other hand zeolite addition did not show any significant change in the pH sensitivity of the ISFET sensors. With these two main results it can be concluded that zeolites definitely have an effect on membrane-enzyme system but transducer.

CHAPTER 5

CONCLUSIONS

In this study, different types of zeolite attachment methods and performances of zeolite attached biosensors were investigated. Several different types of zeolites were used in order to investigate the effect of zeolites on biosensor performances in general.

In the first part of the study, the most efficient methodology to attach zeolite nanocrystals on Si wafer substrates was investigated. For this purpose three different methods were utilized, which are spin coating, ultra sonication and direct attachment. According to the experimental results, direct attachment method was found to be the most efficient method. This method was shown to be successful in forming a monolayer of zeolite A nanocrystals with 200–250 nm size on the Si wafers and thus this method can also be applicable for even smaller sizes of zeolites than 500 nm. Furthermore, zeolite A nanocrystals were shown to be oriented with a face of the cube parallel to the Si surface by the marked predominance of 100 crystallographic indexes.

Compatibility of this method to micro fabrication techniques is also tested. For this purpose direct attachment method is combined with Electron beam lithography. Experiments showed that it is possible to produce precisely

controllable zeolite patterns with the combination of these two techniques. Moreover it is found that the number of zeolite layers can also be controlled with this combination. It was found that the features of the patterned stripes can be as small as the zeolite size. In conclusion, results showed that with direct attachment method, fully covered and perfectly oriented zeolite nanocrystal monolayers can be achievable.

In order to investigate the possible future use of such zeolite attached surfaces in biosensor applications, effect of zeolite particles on biosensor performances was investigated. Different types of zeolite particles were attached to different types of sensor surfaces with the help of polymeric membranes. Performances of standard sensors and zeolite modified sensors were compared. In general, it was observed that different zeolite types with varying parameters, such as Si/Al ratio, morphologies or ion-exchange properties had significant effect on the sensor performances. Also it was found that some of the zeolite modified sensors showed improved performances when compared with the standard sensors. Although, promising results are gathered from the experiments, further investigations should be done to understand the interactions between enzymes, zeolites and sensor surfaces.

REFERENCES

1. L. C. Clark, C. Lyons, *Ann. N.Y. Acad. Sci.* 1962, 102, 29.
2. K. Narasimham, L. B. Wingard, Jr. *Anal. Chem.* 1986, 58, 2984.
3. B. Oisson, H. Lundback, G. Johansson, F. Scheller, J. Nentwig, *Anal. Chem.* 1986, 58, 2984.
4. Y. Degani, A. Heller, *J. Am. Chem. Soc.* 1988, 110, 2615.
5. G. Fortier, M. Vaillancourt, D. Belanger, *Electroanalysis* 1992, 4, 275.
6. P.C. Pandey, *J. Chem. Soc., Faraday Trans.* 1988, 84, 2259.
7. M. Mascini, M. Iannello, G. Palleschi, *Anal. Chim. Acta* 1983, 146, 135.
8. J. Qian, Y. Liu, H. Liu, T. Yu, J. Deng, *J. Electroanal. Chem.* 1995, 397, 157.
9. H.H. Weetall, N.B. Havewala, W.H. Pitcher, C.C. Detar, W.P. Vann, S. Yaverbaum, *Biotechnol. Bioeng.* 1974, 16, 295.
10. Y.Y. Lee, A.R. Fratzke, K. Wun, G.T. Tsao, *Biotechnol. Bioeng.* 1976, 18, 389.
11. D.B. Johnson, D. Thornton, P.D. Ryan, *Biochem. Soc. Trans.* 1974, 2, 494.
12. D. Thornton, M.J. Byrne, A. Flynn, D.B. Johnson, *Biochem. Soc. Trans.* 1974, 2, 1360.

13. D. Thronton, A. Flynn, D.B. Johnson, P.D. Ryan, *Biotechnol. Bioeng.* 1975, **17**, 1679.
14. A. Flynn, D.B. Johnson, *Int. J. Biochem.* 1977, **8**, 501.
15. A. Flynn, D.B. Johnson, *Int. J. Biochem.* 1977, **8**, 243.
16. D. Rolison, *Chem. Rev.* 1990, **90**, 867.
17. K. Mukhopadhyay, S. Phadtare, V. P. Vinod, A. Kumar, M. Rao, R. V. Chaudhari, M. Sastry, *Langmuir* 2003, **19**, 3858-3863.
18. H. Ma, J. He, D. G. Evans, X. Duan, *Journal of Molecular Catalysis B: Enzymatic* 30 (2004) 209–217.
19. G.-W. Xing, X.-W. Li, G.-L. Tian, Y.-H. Ye, *Tetrahedron* 56 (2000) 3517-3522.
20. B. Liu, R. Hu, J. Deng, *Anal. Chem.* 1997, **69**, 2343-2348.
21. Z. Lai, G. Bonilla, I. Diaz, J.G. Nery, K. Sujaoti, M.A. Amat, E. Kokkoli, O. Terasaki, R.W. Thompson, M. Tsapatsis, D.G. Vlachos, *Science* 300 (2003) 456.
22. G.T.P. Mabande, S. Ghosh, Z. Lai, W. Schwieger, M. Tsapatsis, *Ind. Eng. Chem. Res.* 44 (2005) 9086.
23. S. Li, Z. Li, D. Medina, C. Lew, Y. Yan, *Chem. Mater.* 17 (2005) 1851.
24. S. Li, Z. Li, K.N. Bozhilov, Z. Chen, Y. Yan, *J. Am. Chem. Soc.* 126 (2004) 10732.
25. S. Li, J. Sun, J. Li, H. Peng, D. Gidley, E.T. Ryan, Y. Yan, *J. Phys. Chem. B* 108 (2004) 11689.
26. G. Clet, J.C. Jansen, H. van Bekkum, *Chem. Mater.* 11 (1999) 1696.
27. N. van der Puil, F.M. Dautzenberg, H. van Bekkum, J.C. Jansen, *Micropor. Mesopor. Mater.* 27 (1999) 95.

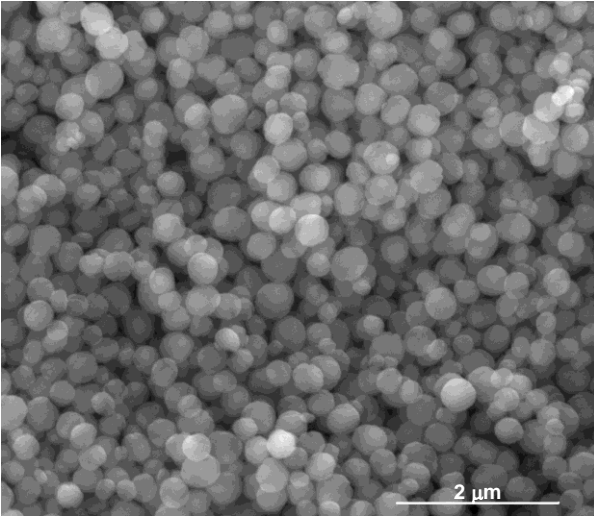
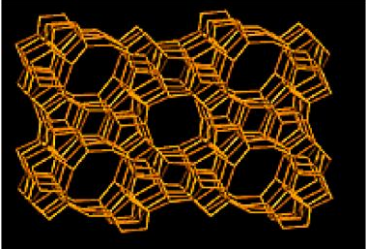
28. Y. Yan, T. Bein, *J. Phys. Chem.* 96 (1992) 9387.
29. Z. Li, C. Lai, T.E. Mallouk, *Inorg. Chem.* 28 (1989) 178.
30. J.-W. Li, K. Pfanner, G. Calzaferri, *J. Phys. Chem.* 99 (1995) 12368.
31. J.-W. Li, G. Calzaferri, *J. Chem. Soc. Chem. Commun.* (1993) 1430.
32. P. Laine', R. Seifert, R. Giovanoli, G. Calzaferri, *New J. Chem.* 21 (1997) 453.
33. G.D. Stucky, J.E. Mac Dougall, *Science* 247 (1990) 669.
34. N.C. Jeong, H.S. Kim, K.B. Yoon, *Langmuir* 21 (2005) 6038.
35. H.S. Kim, S.M. Lee, K. Ha, C.S. Jung, Y.-J. Lee, Y.S. Chun, D.S. Kim, B.K. Rhee, K.B. Yoon, *J. Am. Chem. Soc.* 126 (2004) 673.
36. A. Kulak, Y.-J. Lee, Y.S. Park, K.B. Yoon, *Angew. Chem. Int. Ed.* 39 (2000) 950.
37. S.Y. Choi, Y.-J. Lee, Y.S. Park, K. Ha, K.B. Yoon, *J. Am. Chem.Soc.* 122 (2000) 5201.
38. K. Ha, Y.-J. Lee, H.J. Lee, K.B. Yoon, *Adv. Mater.* 12 (2000) 1114.
39. G.S. Lee, Y.-J. Lee, K.B. Yoon, *J. Am. Chem. Soc.* 123 (2001) 9769.
40. J.S. Park, G.S. Lee, Y.-J. Lee, Y.S. Park, K.B. Yoon, *J. Am. Chem. Soc.* 124 (2002) 13366.
41. J.S. Park, Y.-J. Lee, K.B. Yoon, *J. Am. Chem. Soc.* 126 (2004) 1934.
42. J.S. Lee, K. Ha, Y.-J. Lee, K. B. Yoon, *Adv. Mater.*, 2005, 7(17): 837-840.
43. K.B. Yoon, *Bull. Kor. Chem. Soc.* 27 (2006) 17.
44. T. Ban, T. Ohwaki, Y. Ohya, Y. Takahashi, *Angew. Chem. Int. Ed.* 38 (1999) 3324.

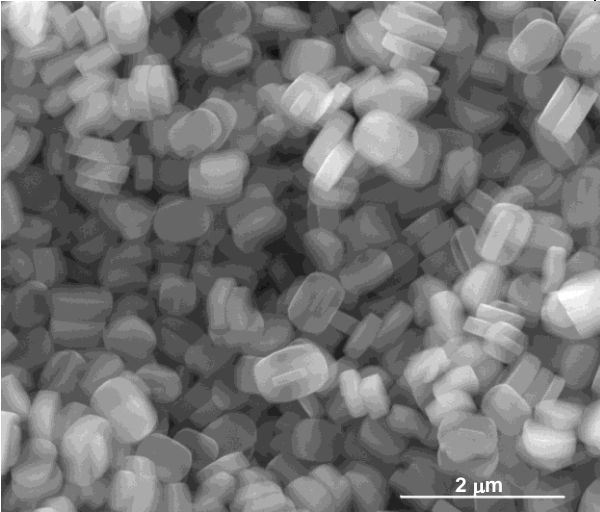
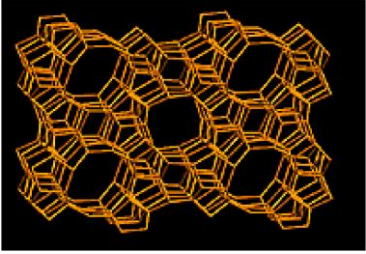
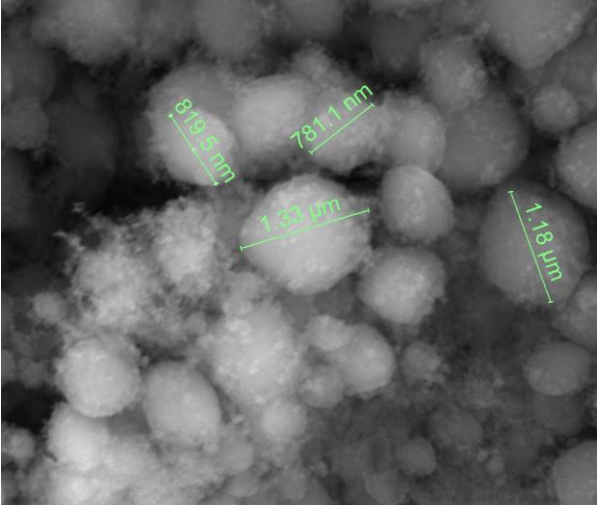
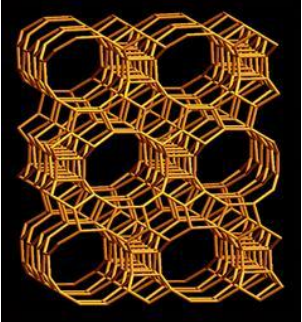
45. L.C. Boudreau, J.A. Kuck, M. Tsapatsis, *J. Membr. Sci.* 152 (1999) 41.
46. K. Ha, Y.-J. Lee, Y.S. Chun, Y.S. Park, G.S. Lee, K.B. Yoon, *Adv. Mater.* 13 (2001) 594.
47. K. Ha, Y.-J. Lee, D.-Y. Jung, J.H. Lee, K.B. Yoon, *Adv. Mater.* 12 (2000) 1614.
48. A. Jakob, V. Valtchev, M. Souillard, D. Faye, *Langmuir* 2009, 25, 3549-3555.
49. M.C. Lovallo, M. Tsapatsis, *AIChE J.*, 1996, 42(11): 3020—3029.
50. S. Mintova, T. Bein, *Adv Mater*, 2001, 13(24): 1880—1883.
51. K.T. Jung, Y.G. Shul, *J Membr Sci*, 2001, 191(1-2): 189—197.
52. J.S. Lee, J.H. Kim, Y.J. Lee, N.C. Jeong, K.B. Yoon, *Angew. Chem. Int. Ed.* 46 (2007) 3087.
53. L. Huang, Y. Yan, D. Zhao, *J Am Chem Soc*, 2000, 122(14): 3530—3531
54. B. Zhang, M. Zhou, X. Liu, *Adv. Mater.* 20 (2008) 2183.
55. M. Zhou, X. Liu, B. Zhang, H. Zhu, *Langmuir* 24 (2008) 11946.
56. A. Kulak, Y.S. Park, Y.-J. Lee, Y. Sung, K. Ha, K.B. Yoon, *J. Am. Chem. Soc.* 122 (2000) 9308.
57. T. Goriushkina, L. Shkotova, G. Gayda, H. Klepach, M. Gonchar, A. Soldatkin, S. Dzyadevych, *Sens. Actuators B: Chemical.* 2008, doi:10.1016/j.snb.2008.11.051.
58. T. Goriushkina, A. Soldatkin, S. Dzyadevych, *J. Agric. Food Chem.* 57 (2009). 6528–6535.
59. P. Frontera, F. Crea, F. Testa, R. Aiello, *J. Porous Mater.* 14 (2007) 325.
60. T. Yu, Y. Zhang, C. You, J. Zhuang, B. Wang, B. Liu, Y. Kang, Y. Tang, *Chem. Eur. J.* 12 (2006) 1137.

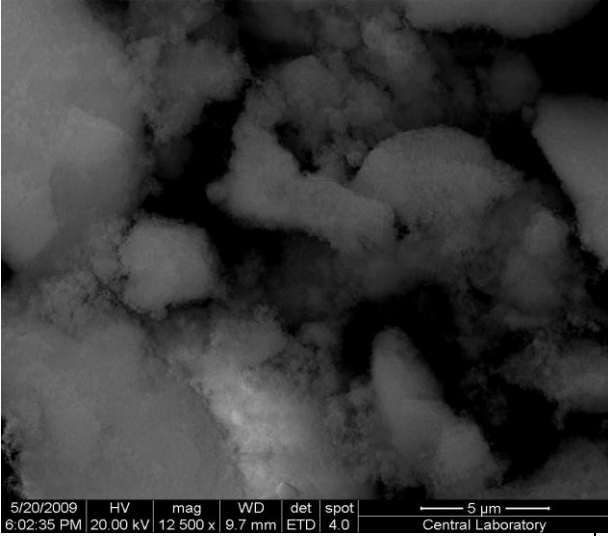
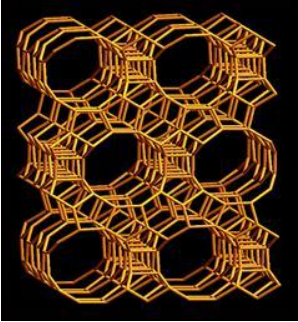
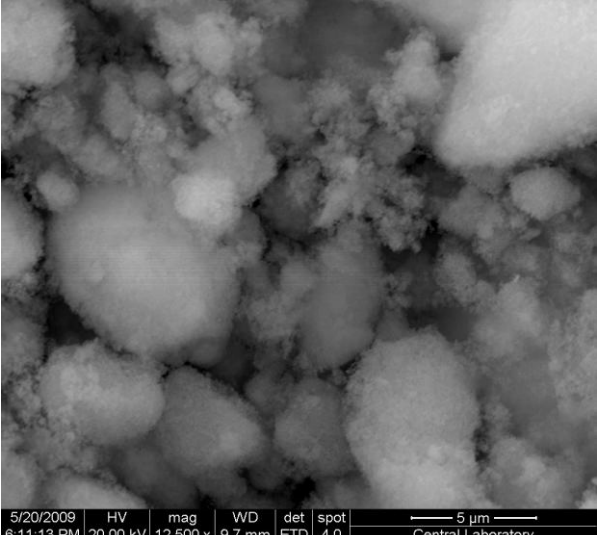
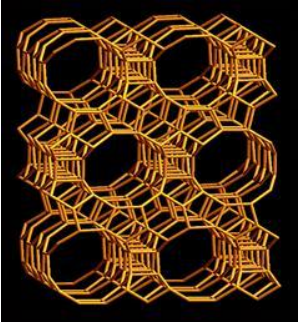
61. H. Lee, J.S. Park, K.B. Yoon, D.H. Kim, S.H. Seo, H.C. Kang, D.Y. Noh, H. Kim, *Thin Solid Films* 515 (2007) 5678.
62. K.B. Yoon, *Acc. Chem. Res.* 40 (2007) 29.
63. F. Cucinotta, Z. Popovic, E.A. Weiss, G.M. Whitesides, L.D. Cola, *Adv. Mater.* 20 (2008) 1.
64. W. Sun, K.F. Lam, L.W. Wong, K.L. Yeung, *Chem. Commun.* (2005) 4911.
65. W. Shan, Y. Zhang, W. Yang, C. Ke, Z. Gaoi, Y. Ye, Y. Tang, *Micropor. Mesopor. Mater.* 69 (2004) 35.
66. K. Sakaguchi, M. Matsui, F. Mizukami, *Appl. Microbiol. Biotechnol.* 67 (2005) 306–311.
67. T. Bein, *Mater. Res. Soc. Bull.* 30 (2005) 713.

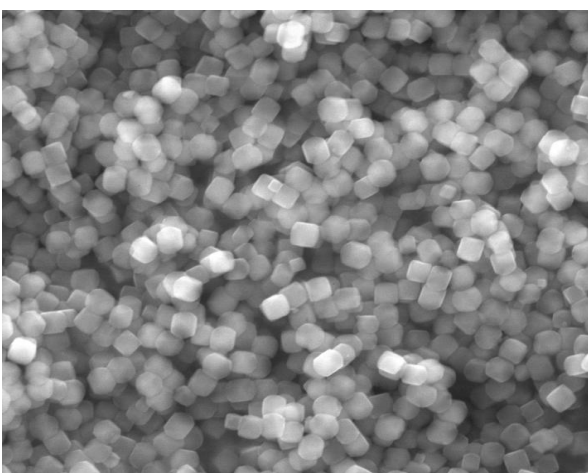
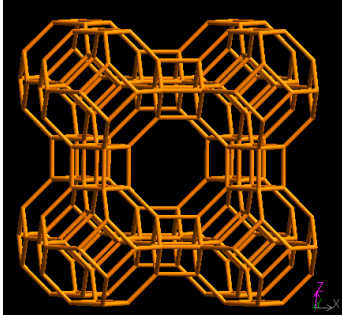
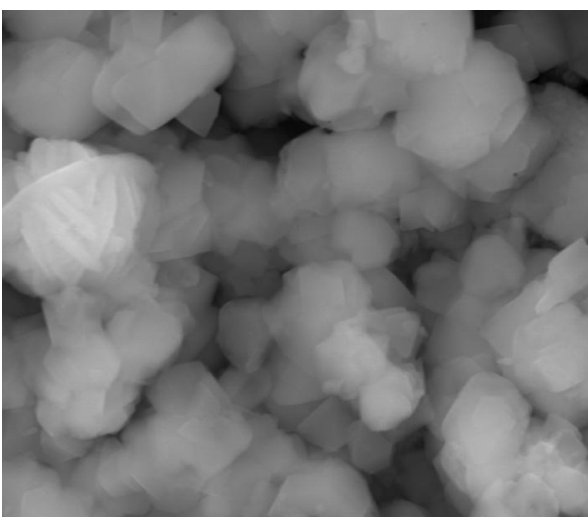
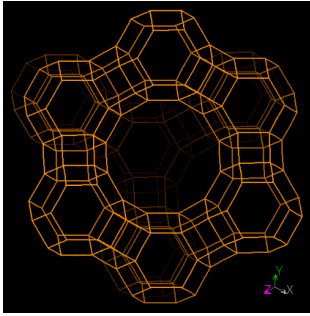
Appendix A

Table of Zeolite samples

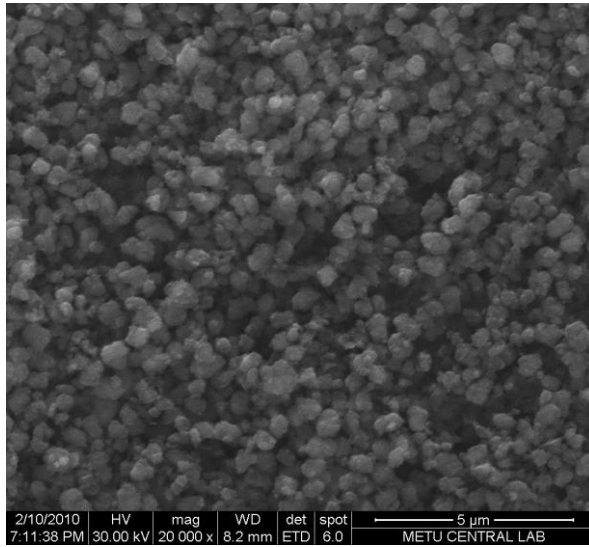
A	 <p>A scanning electron microscope (SEM) image showing a dense collection of spherical Silicalite-1 particles. The particles are uniform in size and densely packed. A scale bar in the bottom right corner of the image indicates a length of 2 μm.</p>	<p>Name: Silicalite-1</p> <p>Si/Al Ratio : All Silicon</p> <p>Gel Formula:</p> <p>1TPAOH:5TEOS:500H₂O</p> <p>Pore Size: 0.53nm x 0.56nm</p> <p>Cristal Structure:</p>  <p>A 3D ball-and-stick model of the Silicalite-1 crystal structure, showing a complex, interconnected network of silicon and oxygen atoms forming a porous framework.</p>
---	--	--

B		<p>Name: Silicalite-2</p> <p>Si/Al Ratio : All Silicon</p> <p>Gel Formula: 1TPAOH:4TEOS:350 H₂O</p> <p>Pore Size: 0.53nm x 0.56nm</p> <p>Cristal Structure:</p> 
C	 <p>5/20/2009 HV mag WD det spot 5:51:53 PM 20.00 kV 50 000 x 9.7 mm ETD 4.0</p> <p>2 μm Central Laboratory</p>	<p>Name: H⁺Beta 300</p> <p>Si/Al Ratio : 150</p> <p>Gel Formula: Commercial</p> <p>Pore Size: 0,76nm x0,64nm</p> <p>Cristal Structure :</p> 

D		<p>Name: H⁺Beta 150</p> <p>Si/Al Ratio :75</p> <p>Gel Formula:</p> <p>Commercial</p> <p>Pore Size: 0,76nm x 0,64nm</p> <p>Cristal Structure :</p> 
E		<p>Name: NH₄⁺Beta 25</p> <p>Si/Al Ratio :12,5</p> <p>Gel Formula:</p> <p>Commercial</p> <p>Pore Size: 0,76nm x 0,64nm</p> <p>Cristal Structure :</p> 

F	 <p>9/25/2009 HV mag WD det spot 3:53:47 PM 30.00 kV 40 000 x 10.7 mm ETD 5.0</p> <p>2 μm Central Laboratory</p>	<p>Name: Zeolite A</p> <p>Si/Al Ratio :~1,35</p> <p>Gel Formula:</p> <p>11.25SiO₂:1.8Al₂O₃:13.4(TMA)₂O:0.6Na₂O:700H₂O.</p> <p>Pore Size: 0,41nm</p> <p>Cristal Structure :</p> 
G	 <p>9/25/2009 HV mag WD det spot 4:05:59 PM 30.00 kV 40 000 x 10.5 mm ETD 5.0</p> <p>2 μm Central Laboratory</p>	<p>Name: Zeolite Y</p> <p>Si/Al Ratio :2,39</p> <p>Gel Formula:</p> <p>Commercial</p> <p>Pore Size: 0,74nm</p> <p>Cristal Structure :</p> 

H



Name: Na⁺Beta-30

Si/Al Ratio :15

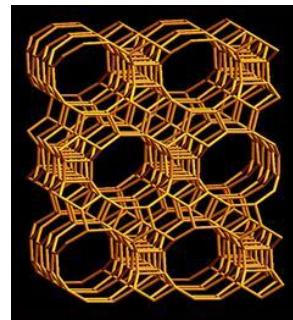
Gel Formula:

1,92 Na₂O : Al₂O₃ : 30 SiO₂ :

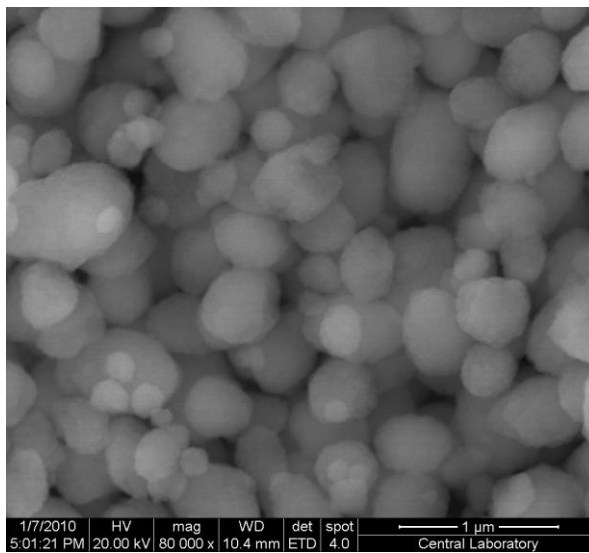
4,6 (TEA)₂O : 444 H₂O

Pore Size: 0,76nm x 0,64nm

Cristal Structure :



I



Name: Na⁺Beta-50

Si/Al Ratio :25

Gel Formula:

1,92 Na₂O : Al₂O₃ : 50 SiO₂ :

4,6 (TEA)₂O : 444 H₂O

Pore Size: 0,76nm x 0,64nm

Cristal Structure :

